PROCEEDINGS A

royalsocietypublishing.org/journal/rspa

Research

Cite this article: Lochner T, Peter MA. 2024 Identification of subwavelength microstructural information from macroscopic boundary measurements in elastodynamics. *Proc. R. Soc. A* **480**: 20240090.
https://doi.org/10.1098/rspa.2024.0090

Received: 2 February 2024
Accepted: 9 October 2024

Subject Category:
Mathematics

Subject Areas:
applied mathematics, differential equations

Keywords:
linearly elastic wave equation, parameter identification, periodic homogenization, shape derivative

Author for correspondence:
Tanja Lochner
e-mail: tanja.lochner@math.uni-augsburg.de

One contribution to a special feature "Mathematical theory and applications of multiple wave scattering" organised by guest editors Luke G. Bennetts, Michael H. Meylan, Malte A. Peter, Valerie J. Pinfield and Olga Umnova.

THE ROYAL SOCIETY PUBLISHING

Identification of subwavelength microstructural information from macroscopic boundary measurements in elastodynamics

Tanja Lochner[1] and Malte A. Peter[1,2]

[1]Institute of Mathematics, University of Augsburg, Augsburg, Germany
[2]Centre for Advanced Analytics and Predictive Sciences, University of Augsburg, Augsburg, Germany

TL, 0000-0003-1962-5724; MAP, 0000-0001-6107-9806

We present a method to obtain microstructural information from macroscopic boundary measurements exploiting scattering governed by the wave equation in a bounded linearly elastic domain in the long-wavelength regime. Applying a force to the outer boundary of the body on the macroscopic scale while measuring the resulting boundary displacement, we solve the inverse problem of identifying the geometry of the microstructure in the context of periodic homogenization minimizing a tracking-type objective functional as long as the geometry of the microstructure is parameterized by a finite set of parameters. Shape calculus is used to characterize the Gâteaux derivative of the objective function facilitating the use of gradient-based algorithms, and we present numerical experiments for a generic non-destructive testing problem for ellipsoidal microstructures showcasing the functioning of the identification method.

1. Introduction

For the durability assessment or quality inspection of structures that owe their properties to microscopic features (porosity patterns, fibre reinforcements, etc.), it is of vital importance to be able to detect damage on

the microscopic scale. As microscopic defects can rarely be measured directly, they have to be identified based on the macroscopic behaviour that they induce, e.g. altered load-bearing capabilities or a changed dynamical response to mechanical excitations. Mathematically, this task gives rise to so-called inverse homogenization problems, i.e. optimization problems governed by multiscale partial differential equations which aim to minimize an objective function depending on macroscopic quantities with respect to a parameter distribution modelling the structure on the microscale.

For a given microstructure, upscaling of the linearly elastic wave equation in three dimensions is a classical result in the context of periodic homogenization assuming scale separation and long wavelengths. The resulting upscaled system is of the same type, where the homogenized (effective) elasticity tensor depends on the macroscopic variable and it is computed from solutions of auxiliary problems stated in the periodicity cell. The homogenized (effective) mass density is obtained by direct averaging.

In order to address the associated inverse problem and deduce from measurements on the boundary the interior geometry of the periodicity cell, we combine the methods of periodic homogenization and parameter identification in this article. Therefore, if measured data of the time-evolution of the deformation of the exterior boundary of a two-scale composite of two solids under given (boundary and/or volume) forcing is available, the results allow us to compute parameters characterizing the microscopic structure under the long-wave assumption, i.e. in the regime where the involved wavelengths are much larger than the characteristic length of the microstructure. Such results are of particular practical relevance if the microstructure is associated with damage (microscopic holes/domains of weak material of a certain size) and our results allow us to compute the extent of the damage (size of the holes/weak domains) from macroscopic boundary measurements.

More concretely, we derive the results on the inverse problem under the assumption that the periodicity cell consists of two perfectly bonded solids, where one part is completely contained in the cell and its geometry is described by a finite vector of real parameters τ. The aim of this paper is then to investigate the minimization problem

$$\operatorname*{argmin}_{\tau \in K} \mathcal{J}(\tau) := \operatorname*{argmin}_{\tau \in K} \frac{1}{2} \|u[\tau] - u_{\mathrm{m}}\|^2_{S \times [L^2(\partial\Omega)]^3},$$

where the parameter vector $\tau \in K$, $K \subset \mathbb{R}^N$ compact, parameterizes the geometry of the microstructure, $u[\tau]: S \times \Omega \to \mathbb{R}^3$ is the displacement field for given τ and u_{m} is the measured displacement. Besides proving the well-posedness of the inverse problem, we characterize the Gâteaux derivative of the objective function making use of shape calculus, which facilitates the use of gradient-based algorithms for finding the optimal τ numerically.

The associated stationary (elliptic) problem has recently been solved in [1] and we make use of the results presented therein for the elliptic part of our time-dependent problem. Besides, the focus in [1] was on an ellipsoidal microstructure, which we extend to general microstructures parameterized by a finite vector throughout this work. In general, the stationary problem has received considerably more attention than the wave-scattering analogue, which is the focus of this article. Most closely related are the works [2] (optimizing textile-materials via homogenization and beam approximation), [3] (homogenization in connection with shape optimization for linearized elasticity in two dimensions) as well as [4] (linear elasticity equation together with some thermal stress tensor). The latter work is also in the setting of inverse homogenization but the method of Céa in connection with a smoothed interface is used instead of a sharp interface as we consider here. It is also worth mentioning [5] who investigate the damage evolution in linear elasticity via shape optimization, whereby they need to compute the shape derivative. They handle the difficulty that the interface moves instead of the outer boundary and the full strain and stress tensors are not continuous across the interface, but this work is not set in a multiscale context. Very recently, related results based on homogenization and shape

optimization were derived by [6] in the context of linear elasticity and by [7] in the context of the Maxwell equations.

The literature on the mathematics of the associated inverse vector-valued wave problem in the long-wavelength limit as it is relevant in the context of bounded volumes of elastic multiscale solids seems very scarce [8]. Nevertheless, there are a number of related works in the context of the time-harmonic scalar wave equation. For example, [9] compute topological sensitivities of the effective parameters due to topological perturbations of a microscopic unit cell based on a two-scale expansion while, in a single-scale context, [10] present a method for elastic-wave identification of discrete heterogeneities based on shape and material sensitivities, i.e. the material parameters are unknown as well, via an adjoint field approach and direct differentiation of the boundary integral equation. Also related, [11] and [12] consider the homogenization of a transmission problem arising in the scattering theory for bounded inhomogeneities with periodic coefficients modelled by the anisotropic Helmholtz equation and also discuss boundary correctors. As the inverse problem considered in this paper focuses on bounded volumes of elastic multiscale solids, it is closely related to engineering problems in non-destructive testing, cf. e.g. [13,14]. Also note that the different regime, in which the wavelength is of comparable size to the microstructure, is highly relevant in optics (imaging). Some more general results in shape optimization by homogenization method can be found in the books of e.g. Allaire [15] and Delfour & Zolesio [16] and in the theory of inverse problems of e.g. Isakov [17] and Kirsch [18].

The article is organized as follows: In §2, we introduce the forward two-scale problem, discuss its homogenization limit and briefly summarize the existence and uniqueness of the solutions. In §3, we formulate the inverse problem and show the existence of at least one solution of the inverse problem (§3a). After computation of the Gâteaux derivative of the homogenized tensor, we derive the Gâteaux derivative of the objective functional of the inverse problem (§3b). For example microstructures consisting of ellipsoids, some numerical experiments showcase the functioning of the method in §4. Conclusions are drawn in §5.

2. The homogenized direct problem

Let $S = (0, T)$ with $0 < T < \infty$, $\Omega \subset \mathbb{R}^3$ be an open bounded connected Lipschitz-domain, $\Gamma_D \subset \partial\Omega$ closed with $|\Gamma_D| > 0$, $\Gamma_N = \partial\Omega \setminus \Gamma_D$ and $Y = (0, l_1) \times (0, l_2) \times (0, l_3) \subset \mathbb{R}^3$ with $l_1, l_2, l_3 > 0$. We define the Banach spaces

$$H^1_{\Gamma_D}(\Omega) := \left\{ u \in [H^1(\Omega)]^3 \mid u = 0 \text{ on } \Gamma_D \right\} \quad \text{and} \quad L^2_\varrho(\Omega) := [L^2(\Omega)]^3$$

equipped with norms

$$\|u\|_{H^1_{\Gamma_D}(\Omega)} = \|e(u)\|_{[L^2(\Omega)]^{3\times 3}} \quad \text{and} \quad \|u\|_{L^2_\varrho(\Omega)} = \sqrt{\langle u, u\rangle_\varrho},$$

where $e(u) = \frac{1}{2}(\nabla u + (\nabla u)^T)$ and $\langle \cdot, \cdot \rangle_\varrho$ is the weighted scalar product $\langle u, v\rangle_\varrho = \int_\Omega \varrho(x) u(x) v(x) \mathrm{d}x$ for pairs of functions in the space $L^2_\varrho(\Omega) \times L^2_\varrho(\Omega)$ with $0 < \varrho \in L^\infty(\Omega)$. Using Korn's inequality for functions with zero value on part of the boundary [19, Korollar 25.6], $\|\cdot\|_{H^1_{\Gamma_D}(\Omega)}$ defines a norm on the separable Hilbert space $H^1_{\Gamma_D}(\Omega)$. Moreover, we can introduce the associated Gelfand triple

$$H^1_{\Gamma_D}(\Omega) \subset L^2_\varrho(\Omega) = \left(L^2_\varrho(\Omega)\right)^* \subset (H^1_{\Gamma_D}(\Omega))^* .$$

In what follows, we consider bounded sequences $\{(A^\varepsilon, \varrho^\varepsilon)\}$ of (elasticity) tensors A^ε of fourth order in $M(\alpha, \beta, \Omega)$ (see definition 2.1) and (mass density) functions ϱ^ε in $L^\infty(\Omega)$, which satisfy $0 < \varrho_0 < \varrho^\varepsilon(x) < \varrho_1$ for some $\varrho_0, \varrho_1 \in \mathbb{R}$ and for a.e. $x \in \Omega$.

Definition 2.1. *Let $\alpha, \beta \in \mathbb{R}$ with $0 < \alpha < \beta$ and let $\mathcal{O}$ be an open set in $\mathbb{R}^3$. We denote by $M(\alpha, \beta, \mathcal{O})$ the set of all tensors $B = (b_{ijkh})_{1 \le i,j,k,h \le 3}$ such that*

royalsocietypublishing.org/journal/rspa Proc. R. Soc. A 480: 20240090

(i) $b_{ijkh} \in L^\infty(\mathcal{O})$ for all $i, j, k, h \in \{1, 2, 3\}$,
(ii) $b_{ijkh} = b_{jikh} = b_{khij}$ for all $i, j, k, h \in \{1, 2, 3\}$,
(iii) $\alpha|m|^2 \le Bmm$ for all symmetric matrices m,
(iv) $|B(x)m| \le \beta|m|$ for all matrices m,

a.e. in $\mathcal{O}$, where

$$\begin{cases} Bm := \left((Bm)_{ij}\right)_{1\le i,j\le 3} = \left(\left(\sum_{k,h=1}^3 B_{ijkh} m_{kh}\right)_{ij}\right)_{1\le i,j\le 3}, \\ Bm\tilde{m} := \sum_{i,j,k,h=1}^3 b_{ijkh} m_{ij} \tilde{m}_{kh}, \\ |m| := \left(\sum_{i,j=1}^3 m_{ij}^2\right)^{\frac{1}{2}}, \end{cases}$$

for quadratic matrices $m = \left(m_{ij}\right)_{1\le i,j\le 3}$ and $\tilde{m} = \left(\tilde{m}_{ij}\right)_{1\le i,j\le 3}$.

We define for every ε the (vector-valued) three-dimensional wave-propagation problem

$$\begin{cases} \partial_t(\varrho^\varepsilon \partial_t u^\varepsilon) - \nabla \cdot (A^\varepsilon e(u^\varepsilon)) = f & \text{in } S \times \Omega, \\ u^\varepsilon = 0 & \text{on } S \times \Gamma_D, \\ A^\varepsilon e(u^\varepsilon)\nu = g & \text{on } S \times \Gamma_N, \\ u^\varepsilon(0, x) = u_0(x) & \text{a.e. in } \Omega, \\ \partial_t u^\varepsilon(0, x) = u_1(x) & \text{a.e. in } \Omega, \end{cases} \tag{2.1}$$

where ν is the outward-pointing normal to Γ_N and f is a given force density (per volume). It can be rewritten as $\varrho^\varepsilon \frac{f}{\varrho^\varepsilon}$ with $\frac{f}{\varrho^\varepsilon}$ force per mass, which is well-defined since $0 < \varrho_0 < \varrho^\varepsilon$. Thus, we can prove the existence and uniqueness of the weak solution.

Theorem 2.1. *Let $(A^\varepsilon, \varrho^\varepsilon)$ be defined as above, $u_0 \in H^1_{\Gamma_D}(\Omega)$, $u_1 \in [L^2(\Omega)]^3$, $f \in [L^2(S \times \Omega)]^3$ and $g \in H^1(S; [L^2(\Gamma_N)]^3)$. Then, there exists a unique weak solution $u^\varepsilon \in L^2(S; H^1_{\Gamma_D}(\Omega))$ of (2.1) with $u^\varepsilon \in L^\infty(S; H^1_{\Gamma_D}(\Omega))$, $\partial_t u^\varepsilon \in L^\infty(S; [L^2(\Omega)]^3)$ and $\partial_t(\varrho^\varepsilon \partial_t u^\varepsilon) \in L^2(S; (H^1_{\Gamma_D}(\Omega))^*)$ in the sense of distributions, as well as $u^\varepsilon \in C^0(\overline{S}; [L^2(\Omega)]^3)$, i.e. for all $v \in L^2(S; H^1_{\Gamma_D}(\Omega))$ with $\partial_t v \in L^2(S; L^2_{\varrho^\varepsilon}(\Omega))$ and $v(T) = 0$ there holds*

$$\begin{aligned} &-\int_0^T \int_\Omega \varrho^\varepsilon \partial_t u^\varepsilon \cdot \partial_t v \, \mathrm{d}x\mathrm{d}t + \int_0^T \int_\Omega A^\varepsilon e(u^\varepsilon) e(v) \, \mathrm{d}x\mathrm{d}t \\ &\qquad = \int_0^T \int_\Omega f \cdot v \, \mathrm{d}x\mathrm{d}t + \int_0^T \int_{\Gamma_N} g \cdot v \, \mathrm{d}\sigma(x)\mathrm{d}t + \int_\Omega \varrho^\varepsilon u_1 \cdot v(0) \, \mathrm{d}x \end{aligned} \tag{2.2}$$

and $u^\varepsilon(0) = u_0$. Furthermore,

$$\begin{aligned} &\|u^\varepsilon\|^2_{L^\infty(S; H^1_{\Gamma_D}(\Omega))} + \|\partial_t u^\varepsilon\|^2_{L^\infty(S; [L^2(\Omega)]^3)} \\ &\qquad \le C\left(\|u_1\|^2_{[L^2(\Omega)]^3} + \|u_0\|^2_{H^1_{\Gamma_D}(\Omega)} + \|f\|^2_{L^2(S; [L^2(\Omega)]^3)} + \|g\|^2_{H^1(S; [L^2(\Gamma_N)]^3)}\right) \end{aligned} \tag{2.3}$$

for some constant C independent of ε.

Proof. The existence and uniqueness result is standard. For example, it can be proven similarly as [19, Theorem 12.4] by using the Galerkin method. As part of such an existence proof, it is necessary to show *a priori* estimates similar to (2.3) independent of the Galerkin-approximation parameter. Some care has to be taken in order to derive the ε-independent estimates (2.3), which are necessary for the homogenization process below. From the standard results, we obtain the estimate

$$\begin{aligned} &\|u\|^2_{L^\infty(S; H^1_{\Gamma_D}(\Omega))} + \|\partial_t u\|^2_{L^\infty(S; L^2_{\varrho^\varepsilon}(\Omega))} \\ &\qquad \le C\left(\|u_1\|^2_{L^2_{\varrho^\varepsilon}(\Omega)} + \|u_0\|^2_{H^1_{\Gamma_D}(\Omega)} + \|\frac{1}{\varrho^\varepsilon} f\|^2_{L^2(S; L^2_{\varrho^\varepsilon}(\Omega))} + \|g\|^2_{H^1(S; [L^2(\Gamma_N)]^3)}\right). \end{aligned} \tag{2.4}$$

Using the assumption on ϱ^ε, we have

$$\sqrt{\varrho_0}\|u\|_{[L^2(\Omega)]^3} \le \|u\|_{L^2_{\varrho^\varepsilon}(\Omega)} \le \sqrt{\varrho_1}\|u\|_{[L^2(\Omega)]^3},$$

which we can apply on (2.4) to get (2.3). ∎

Under the assumptions of theorem 2.1 and since $L^\infty(S; H^1_{\Gamma_D}(\Omega)) \subset L^2(S; H^1_{\Gamma_D}(\Omega))$ and $L^\infty(S; [L^2(\Omega)]^3) \subset [L^2(S\times\Omega)]^3$, we get the weak convergences

$$u^\varepsilon \rightharpoonup u \text{ in } L^2(S; H^1_{\Gamma_D}(\Omega)) \quad \text{and} \quad \partial_t u^\varepsilon \rightharpoonup \partial_t u \text{ in } [L^2(S\times\Omega)]^3. \tag{2.5}$$

We split the domain Ω in two disjoint sets depending on $\varepsilon > 0$, namely $\Omega^\varepsilon := \text{interior}\left(\bigcup_{\xi\in\Lambda^\varepsilon} \varepsilon(\overline{Y}+\xi)\right)$, where $\Lambda^\varepsilon := \{\xi \in \mathbb{R}^3 : \varepsilon(Y+\xi) \subset \Omega\}$, and $\Pi^\varepsilon := \Omega\setminus\Omega^\varepsilon$ to introduce the partial periodic unfolding operator $\mathcal{T}^\varepsilon_Y$ from [20, chapter 1.5].

Definition 2.2. *For a Lebesgue-measurable function ϕ on $S\times\Omega$, the partial periodic unfolding operator $\mathcal{T}^\varepsilon_Y : L^p(S\times\Omega) \to L^p(S\times\Omega\times Y)$, $p\in[1,\infty)$, is defined as*

$$\mathcal{T}^\varepsilon_Y(\phi)(t,x,y) = \begin{cases} \phi(t, \varepsilon\left[\frac{x}{\varepsilon}\right] + \varepsilon y) & \text{for a.e. } (t,x,y) \in S\times\Omega^\varepsilon\times Y, \\ 0 & \text{for a.e. } (t,x,y) \in S\times\Pi^\varepsilon\times Y. \end{cases}$$

For functions independent of time, we can use the standard periodic unfolding operator $\mathcal{T}^\varepsilon$ defined in [20, chapter 1.1].

Definition 2.3. *For a Lebesgue-measurable function ϕ on Ω, the periodic unfolding operator $\mathcal{T}^\varepsilon : L^p(\Omega) \to L^p(\Omega\times Y)$, $p\in[1,\infty)$, is defined as*

$$\mathcal{T}^\varepsilon(\phi)(x,y) = \begin{cases} \phi(\varepsilon\left[\frac{x}{\varepsilon}\right] + \varepsilon y) & \text{for a.e. } (x,y) \in \Omega^\varepsilon\times Y, \\ 0 & \text{for a.e. } (x,y) \in \Pi^\varepsilon\times Y. \end{cases}$$

We define $H^1_{\text{per},0}(Y)$ as the space of Y-periodic H^1-functions with zero mean value over Y. The following compactness results apply.

Theorem 2.2. *Let $\{u^\varepsilon\}$ be a sequence with $u^\varepsilon \in L^\infty(S; H^1_{\Gamma_D}(\Omega))$, $\partial_t u^\varepsilon \in L^\infty(S; [L^2(\Omega)]^3)$, $u^\varepsilon(0) = u_0$ and*

$$\|u^\varepsilon\|^2_{L^2(S; H^1_{\Gamma_D}(\Omega))} + \|\partial_t u^\varepsilon\|^2_{\left[L^2(S\times\Omega)\right]^3} \le C$$

for a constant C independent of ε. Then, there exist a subsequence (again denoted by ε), $u \in L^2(S; H^1_{\Gamma_D}(\Omega)) \cap H^1(S; [L^2(\Omega)]^3)$ with $u(0) = u_0$ and $\hat{u} \in L^2(S\times\Omega; [H^1_{\text{per},0}(Y)]^3)$ such that

$$\mathcal{T}^\varepsilon_Y(u^\varepsilon) \rightharpoonup \mathrm{u} \text{ weakly in } [L^2(S\times\Omega\times Y)]^3, \tag{2.6}$$

$$\mathcal{T}^\varepsilon_Y(\partial_t u^\varepsilon) \rightharpoonup \partial_t \mathrm{u} \text{ weakly in } [L^2(S\times\Omega\times Y)]^3, \tag{2.7}$$

$$\mathcal{T}^\varepsilon_Y(\nabla_x u^\varepsilon) \rightharpoonup \nabla u + \nabla_y \hat{u} \text{ weakly in } [L^2(S\times\Omega\times Y)]^{3\times 3}. \tag{2.8}$$

Proof. Using standard estimates of the norm of the partial periodic unfolding operator (cf. [20, proposition 1.50]) and the uniform boundedness of u^ε, we obtain (2.6) and (2.7). The condition $u(0) = u_0$ follows directly from $u^\varepsilon(0) = u_0$ for all $\varepsilon > 0$. Application of [20, proposition 1.50] shows (2.8). ∎

For future reference, we define the mean value of an integrable function $u: S\times\Omega\times Y \to \mathbb{R}$ over the reference cell as

$$\mathcal{M}_Y(u) := \frac{1}{|Y|}\int_Y u(t,x,y)\,\mathrm{d}x. \tag{2.9}$$

Since, by [20, proposition 1.50], $u^\varepsilon \rightharpoonup \mathcal{M}_Y(u) = u$ weakly in $[L^2(S\times\Omega)]^3$ in theorem 2.2, the limit function u coincides with u from (2.5). In the next step, we want to pass to the limit $\varepsilon \to 0$ in (2.2).

Theorem 2.3. *Let* $\{(A^\varepsilon, \varrho^\varepsilon)\}$ *be defined as above,* $f \in [L^2(S\times\Omega)]^3$, $g \in H^1(S; [L^2(\Gamma_N)]^3)$, $u_0 \in H^1_{\Gamma_D}(\Omega)$, $u_1 \in [L^2(\Omega)]^3$ *and* $\{u^\varepsilon\}$ *the associated sequence of weak solutions of* (2.2). *Then, the weak convergences* (2.5), (2.6), (2.7) *and* (2.8) *hold. Suppose that*

$$B^\varepsilon := \mathcal{T}^\varepsilon(A^\varepsilon) \to B \quad \text{and} \quad \mathcal{T}^\varepsilon(\varrho^\varepsilon) \to \varrho$$

a.e. in $\Omega\times Y$. *Then,* $B \in M(\alpha,\beta,\Omega\times Y)$, $0<\varrho_0\le\varrho(x)\le\varrho_1$ *for a.e.* $x\in\Omega$ *and the pair*

$$(u,\hat{u}) \in L^2(S; H^1_{\Gamma_D}(\Omega)) \times L^2(S\times\Omega; [H^1_{\mathrm{per},0}(Y)]^3)$$

with $\partial_t u \in [L^2(S\times\Omega)]^3$ *and* $u(0) = u_0$ *is the weak solution of*

$$\begin{aligned}
&-\int_0^T \int_\Omega \frac{1}{|Y|}\int_Y \varrho(x,y)\,\mathrm{d}y\,\partial_t u(t,x)\cdot\partial_t v(t,x)\,\mathrm{d}x\mathrm{d}t\\
&\quad+\frac{1}{|Y|}\int_0^T\int_{\Omega\times Y} B(x,y)(e(u)(t,x)+e_y(\hat{u})(t,x,y))(e(v)(t,x)+e_y(\hat{v})(t,x,y))\,\mathrm{d}x\mathrm{d}y\mathrm{d}t\\
&=\int_0^T\int_\Omega f(t,x)\cdot v(t,x)\,\mathrm{d}x\mathrm{d}t+\int_0^T\int_{\Gamma_N} g\cdot v(t,x)\,\mathrm{d}\sigma(x)\mathrm{d}t\\
&\quad+\int_\Omega\frac{1}{|Y|}\int_Y \varrho(x,y)\,\mathrm{d}y\,u_1(x)\cdot v(0,x)\,\mathrm{d}x
\end{aligned} \tag{2.10}$$

for all $v \in L^2(S; H^1_{\Gamma_D}(\Omega))$ *with* $\partial_t v \in [L^2(S\times\Omega)]^3$, $v(T)=0$ *and* $\hat{v} \in L^2(S\times\Omega; [H^1_{\mathrm{per},0}(Y)]^3)$.

Proof. The convergences (2.5)–(2.8) follow directly from (2.3) and theorem 2.2. The assumption on B^ε implies that $B \in M(\alpha,\beta,\Omega\times Y)$. Since $0<\varrho_0<\varrho^\varepsilon(x)<\varrho_1$ for a.e. $x\in\Omega$ clearly $0<\varrho_0\le\varrho(x,y)\le\varrho_1$ for a.e. $(x,y)\in\Omega\times Y$. We rewrite the weak formulation (2.2) using the (partial) periodic unfolding operator

$$\begin{aligned}
&-\frac{1}{|Y|}\int_0^T\int_{\Omega\times Y}\mathcal{T}^\varepsilon(\varrho^\varepsilon)\mathcal{T}^\varepsilon_Y(\partial_t u^\varepsilon)\cdot\mathcal{T}^\varepsilon_Y(\partial_t v)\,\mathrm{d}x\mathrm{d}y\mathrm{d}t\\
&\quad+\frac{1}{|Y|}\int_0^T\int_{\Omega\times Y}\mathcal{T}^\varepsilon(A^\varepsilon)\mathcal{T}^\varepsilon_Y(e(u^\varepsilon))\mathcal{T}^\varepsilon_Y(e(v))\,\mathrm{d}x\mathrm{d}y\mathrm{d}t+\mathcal{I}_1\\
&=\frac{1}{|Y|}\int_0^T\int_{\Omega\times Y}\mathcal{T}^\varepsilon_Y(f)\cdot\mathcal{T}^\varepsilon_Y(v)\,\mathrm{d}x\mathrm{d}y\mathrm{d}t+\int_0^T\int_{\Gamma_N} g\cdot v\,\mathrm{d}\sigma(x)\mathrm{d}t\\
&\quad+\frac{1}{|Y|}\int_{\Omega\times Y}\mathcal{T}^\varepsilon(\varrho^\varepsilon)\mathcal{T}^\varepsilon(u_1)\cdot\mathcal{T}^\varepsilon(v(0))\,\mathrm{d}x\mathrm{d}y+\mathcal{I}_2,
\end{aligned} \tag{2.11}$$

where

$$\begin{aligned}
\mathcal{I}_1 &= -\int_0^T\int_{\Pi^\varepsilon}\varrho^\varepsilon\partial_t u^\varepsilon\cdot\partial_t v\,\mathrm{d}x\mathrm{d}t+\int_0^T\int_{\Pi^\varepsilon}A^\varepsilon e(u^\varepsilon)e(v)\,\mathrm{d}x\mathrm{d}t,\\
\mathcal{I}_2 &= \int_0^T\int_{\Pi^\varepsilon} f\cdot v\,\mathrm{d}x\mathrm{d}t+\int_{\Pi^\varepsilon}\varrho^\varepsilon u_1\cdot v(0)\,\mathrm{d}x.
\end{aligned}$$

In the first step, we choose the test function as $v(t,x)=\varphi(t)w(x)$ with $\varphi\in C^1_c([0,T))$ and $w\in\mathcal{D}_{\Gamma_D}(\overline{\Omega})=\{\phi\in[C^\infty(\Omega)]^3 : v \text{ is equal to 0 in a neighbourhood of } \Gamma_D\}$ and pass to the limit, whereby we utilize that the terms $\mathcal{I}_1$ and $\mathcal{I}_2$ vanish because of Hölder's inequality and the fact that

$$\int_{\Pi^\varepsilon}|v|^2\,\mathrm{d}x,\ \int_{\Pi^\varepsilon}|\partial_t v|^2\,\mathrm{d}x,\ \int_{\Pi^\varepsilon}|e(v)|^2\,\mathrm{d}x,\ \int_{\Pi^\varepsilon}|v(0)|^2\,\mathrm{d}x\to 0.$$

royalsocietypublishing.org/journal/rspa Proc. R. Soc. A 480: 20240090

In the second step, we choose $v(t,x) = \varepsilon\varphi(t)\widehat{w}^{\varepsilon}(x)$ with $\widehat{w}^{\varepsilon}(x) = \widehat{w}(x, \frac{x}{\varepsilon})$, where

$$\widehat{w}(x,y) = (\psi_i(x)\eta_i(y))_{1\le i\le 3}$$

and $\varphi \in C_c^\infty(S)$, $\psi \in \mathcal{D}(\Omega)$ and $\eta \in [H^1_{\mathrm{per},0}(Y)]^3$, and pass to limit. Adding both limit equations and using the fact that $C_c^1([0,T)) \otimes \mathcal{D}_{\Gamma_D}(\Omega)$ is dense in $L^2(S; H^1_{\Gamma_D}(\Omega))$ (cf. theorem 3.1 from [21]) and $C_c^\infty(S) \otimes (\mathcal{D}(\Omega) \otimes H^1_{\mathrm{per},0}(Y))^3$ dense in $L^2(S\times\Omega; [H^1_{\mathrm{per},0}(Y)]^3)$, we obtain (2.10).

We can reformulate the homogenized problem (2.10) as a macroscopic problem with some homogenized elasticity tensor defined via auxiliary cell problems by splitting the problem.

Theorem 2.4. *The solution u of the homogenized problem (2.10) is also the solution to the following problem: Find $u \in L^2(S; H^1_{\Gamma_D}(\Omega))$ with $\partial_t u \in [L^2(S\times\Omega)]^3$ and $u(0) = u_0$ such that*

$$\begin{aligned} &-\int_0^T\int_\Omega \mathcal{M}_Y(\varrho(x,\cdot))\partial_t u(t,x)\cdot\partial_t v(t,x)\,\mathrm{d}x\mathrm{d}t + \int_0^T\int_\Omega A^{\mathrm{hom}}(x)e(u)(t,x)e(v)(t,x)\,\mathrm{d}x\mathrm{d}t \\ &= \int_0^T\int_\Omega f(t,x)\cdot v(t,x)\,\mathrm{d}x\mathrm{d}t + \int_0^T\int_{\Gamma_N} g\cdot v(t,x)\,\mathrm{d}\sigma(x)\mathrm{d}t + \int_\Omega \mathcal{M}_Y(\varrho(x,\cdot))u_1(x)\cdot v(0,x)\,\mathrm{d}x \end{aligned} \tag{2.12}$$

for all $v \in L^2(S; H^1_{\Gamma_D}(\Omega))$ with $\partial_t v \in [L^2(S\times\Omega)]^3$ and $v(T) = 0$, where $A^{\mathrm{hom}} = (a^{\mathrm{hom}}_{ijkl})_{1\le i,j,k,l\le 3}$ with

$$a^{\mathrm{hom}}_{ijkl}(x) = \frac{1}{|Y|}\int_Y B(x,y)e_{ij}(e_{kl} - e_y(w^{kl})(x,y))\mathrm{d}y$$

for a.e. $x \in \Omega$, where the e_{kl} constitute the canonical basis of symmetric matrices and $w^{kl} \in [L^\infty(\Omega, H^1_{\mathrm{per},0}(Y))]^3$, $k,l \in \{1,2,3\}$, is the unique solution of the cell problem

$$\int_Y B(x,y)\big(e_y(w^{kl})(\,\cdot\,,y) - e_{kl}\big)e_y(v)(y)\mathrm{d}y = 0 \tag{2.13}$$

for all $v \in [H^1_{\mathrm{per},0}(Y)]^3$.

Proof. This result follows by standard arguments. It can be shown as in the proof of [20, proposition 3.7] for the diffusion problem.

We know from [1, theorem 4] that $A^{\mathrm{hom}} \in M(\alpha, \beta^2/2, \Omega)$ if B is Y-periodic in the second argument. Using this, we can prove the uniqueness of the solution to the homogenized problem.

Theorem 2.5. *Let B be Y-periodic in the second argument. Then, there exists a unique solution $u \in L^2(S; H^1_{\Gamma_D}(\Omega))$ with $\partial_t u \in [L^2(S\times\Omega)]^3$ and $u(0) = u_0$ of problem (2.12).*

Proof. We assume that there exist two weak solutions u_a and u_b. Owing to the linearity, there holds $u(0) = 0$ for $u = u_a - u_b$ and

$$-\int_0^T\int_\Omega \mathcal{M}_Y(\varrho(x,\cdot))\partial_t u(t,x)\cdot\partial_t v(t,x)\,\mathrm{d}x\mathrm{d}t + \int_0^T\int_\Omega A^{\mathrm{hom}}(x)e(u)(t,x)e(v)(t,x)\,\mathrm{d}x\mathrm{d}t = 0$$

for all $v \in L^2(S; H^1_{\Gamma_D}(\Omega))$ with $\partial_t v \in [L^2(S\times\Omega)]^3$ and $v(T) = 0$. Let $0 \le s \le T$, χ_s the characteristic function of the interval $[0,s]$ and

$$v(t,x) = \int_0^t \chi_s(\tau)u(\tau,x)\,\mathrm{d}\tau - \int_0^T \chi_s(\tau)u(\tau,x)\,\mathrm{d}\tau\,.$$

Then, v is an admissible test function, $v(t,\,\cdot\,) = v(T,\,\cdot\,) = 0$ for $s \le t \le T$, v is absolutely continuous in $[0,T]$ and $\partial_t v(t,x) = \chi_s(t)u(t,x)$ a.e. in $S\times\Omega$. Using the definition of v as well as the symmetry and coercivity of A^{hom}, we obtain

royalsocietypublishing.org/journal/rspa Proc. R. Soc. A 480: 20240090

$$0 = \int_0^s \int_\Omega \mathcal{M}_Y(\varrho(x,\cdot))\partial_t u(t,x)\cdot u(t,x)\,\mathrm{d}x\mathrm{d}t + \frac{1}{2}\int_\Omega A^{\mathrm{hom}}(x)e(v)(0,x)e(v)(0,x)\,\mathrm{d}x$$
$$\geq \frac{1}{2}\varrho_0\|u(s,\cdot)\|^2_{[L^2(\Omega)]^3} + \frac{\alpha}{2}\|v(0,\cdot)\|^2_{H^1_{\Gamma_D}(\Omega)}$$

for a.e. $s \in S$. Thus, $u = 0$, i.e. $u_a = u_b$ a.e. ∎

For future reference, we note that the strong formulation of (2.12) is given by

$$\begin{cases} \partial_t(\mathcal{M}_Y(\varrho)\partial_t u) - \nabla\cdot(A^{\mathrm{hom}}e(u)) &= f & \text{in } S\times\Omega,\\ u &= 0 & \text{on } S\times\Gamma_D,\\ (A^{\mathrm{hom}}e(u))\cdot\nu &= g & \text{on } S\times\Gamma_N,\\ u(0,x) &= u_0(x) & \text{a.e. in } \Omega,\\ \partial_t u(0,x) &= u_1(x) & \text{a.e. in } \Omega. \end{cases}$$

3. Inverse problem

Having solved the multiscale forward problem and characterized its solution in terms of the homogenized problem given in theorem 2.4, we now turn to the inverse problem of identifying the unknown geometry of the microstructure for a material made up of two constituent materials mixed on the fine scale from macroscopic measurements.

More concretely, for the inverse problem, we assume that the reference cell $Y = (0,l_1)\times(0,l_2)\times(0,l_3) \subset \mathbb{R}^3$ with $l_1, l_2, l_3 > 0$ can be separated into two parts, where one is a Lipschitz domain Y_0 with $|Y_0| > 0$ completely contained in Y, whose domain can be described by a (finite) vector of real parameters $\tau \in K$ with $K \subset \mathbb{R}^N$ compact, and $Y_1 := Y \setminus Y_0$. To emphasize that the structure in the cuboid Y depends on τ, we write $Y[\tau]$, $Y_0[\tau]$ and $Y_1[\tau]$ instead of Y, Y_0, Y_1 in what follows. We consider an elasticity tensor $A^\varepsilon[\tau]$ of the form

$$A^\varepsilon[\tau](x) = A^0(x)\chi_{Y_0[\tau]}\left(\frac{x}{\varepsilon}\right) + A^1(x)\chi_{Y_1[\tau]}\left(\frac{x}{\varepsilon}\right)$$

with $\chi_{Y_0[\tau]}$ (respectively, $\chi_{Y_1[\tau]}$) the characteristic function of the Y-periodically extended domain $Y_0[\tau]$ (respectively, $Y_1[\tau]$) and some fourth-order tensors $A^0, A^1 \in M(\alpha,\beta,\Omega)$ such that

$$\mathcal{T}^\varepsilon(A^\varepsilon[\tau])(x,y) \to A^0(x)\chi_{Y_0[\tau]}(y) + A^1(x)\chi_{Y_1[\tau]}(y) =: B[\tau](x,y)$$

for a.e. $(x,y) \in \Omega\times Y$. Since $B[\tau]$ is Y-periodic, $A^{\mathrm{hom}} = (a^{\mathrm{hom}}_{ijkl})_{1\leq i,j,k,l\leq 3} \in M(\alpha, \frac{\beta^2}{\alpha}, \Omega)$ with

$$a^{\mathrm{hom}}_{ijkl}[\tau](x) = \frac{1}{|Y|}\int_{Y_0[\tau]} A^0(x)e_{ij}(e_{kl} - e_y(w^{kl})(x,y))\,\mathrm{d}y + \frac{1}{|Y|}\int_{Y_1[\tau]} A^1(x)e_{ij}(e_{kl} - e_y(w^{kl})(x,y))\,\mathrm{d}y.$$

Furthermore, we assume that $\varrho^\varepsilon[\tau]$ is of the form

$$\varrho^\varepsilon[\tau](x) = \varrho_0(x)\chi_{Y_0[\tau]}\left(\frac{x}{\varepsilon}\right) + \varrho_1(x)\chi_{Y_1[\tau]}\left(\frac{x}{\varepsilon}\right)$$

for some $0 < \varrho_0, \varrho_1 \in L^\infty(\Omega)$ such that

$$\mathcal{T}^\varepsilon(\varrho^\varepsilon[\tau])(x,y) \to \varrho_0(x)\chi_{Y_0[\tau]}(y) + \varrho_1(x)\chi_{Y_1[\tau]}(y) =: \varrho[\tau](x,y)$$

for a.e. $(x,y) \in \Omega\times Y$.

In the previous section, we are able to compute easily the displacement field $u[\tau]$ of the homogenized problem if the body and its microstructure (defined by Ω and A^ε, respectively, B) as well as the force densities f, g and the initial values u_0 and u_1 are given. From now on, we only know some measured displacement field data u_m on the exterior boundary under applied volume and boundary forces f and g over some time interval S. With this information, we

want to derive the structure of the reference cell Y. We define the input–output operator, which maps the body and boundary forces and the initial values to the solution of the homogenized problem (2.12).

Definition 3.1. (Input–output operator). *Let*

$$\mathcal{L}_\tau : [L^2(S\times\Omega)]^3 \times H^1(S;[L^2(\Gamma_N)]^3) \times H^1_{\Gamma_D}(\Omega) \times [L^2(\Omega)]^3 \to [L^2(S\times\partial\Omega)]^3$$

with

$$(f, g, u_0, u_1) \mapsto u[\tau]|_{\partial\Omega},$$

where $u[\tau] \in L^2(S; H^1_{\Gamma_D}(\Omega)) \cap H^1(S;[L^2(\Omega)]^3)$ *is the solution of the homogenized problem* (2.12) *for given* τ.

Being a solution operator, this operator satisfies some useful properties.

Theorem 3.1. *The operator* $\mathcal{L}_\tau$ *is linear and continuous. Furthermore,* $u[\tau]$ *satisfies*

$$\|u[\tau]\|^2_{[L^2(S\times\partial\Omega)]^3} \le C\Big(\|u_1\|^2_{[L^2(\Omega)]^3} + \|u_0\|^2_{H^1_{\Gamma_D}(\Omega)} + \|f\|^2_{L^2(S;[L^2(\Omega)]^3)} + \|g\|^2_{H^1(S;[L^2(\Gamma_N)]^3)}\Big)$$

for some constant C *independent of the structure of the reference cell* Y.

Proof. Since $A^{\hom} \in M(\alpha, \frac{\beta^2}{\alpha}, \Omega)$, the estimate of $\|u[\tau]\|^2_{[L^2(S\times\partial\Omega)]^3}$ follows directly by theorem 2.1, the continuity of the trace operator and $L^\infty \subset L^2$ for some constant C depending only on α, β but not on the structure of the periodicity cell Y. ∎

Using the input–output operator, we can formulate the inverse problem as follows.

Definition 3.2. (Inverse problem). *Find* $\tau \in K$ *such that for given measured data* $u_m \in [L^2(S\times\partial\Omega)]^3$, *when forces* (f, g) *are applied and initial conditions* u_0, u_1 *are given,* τ *is the solution to the minimization problem*

$$\operatorname*{argmin}_{\tau\in K} \mathcal{J}(\tau) = \operatorname*{argmin}_{\tau\in K} \frac{1}{2}\|\mathcal{L}_\tau(f, g, u_0, u_1) - u_m\|^2_{[L^2(S\times\partial\Omega)]^3}. \tag{3.1}$$

(a) Existence result

First, we show that there exists at least one solution of the inverse problem (3.1).

Theorem 3.2. *The inverse problem* (3.1) *has at least one optimal solution* $\tau^* \in K$.

Proof. Let $\{\tau_n\}$ be a minimizing sequence in K such that

$$\lim_{n\to\infty} \mathcal{J}(\tau_n) = \inf\{\mathcal{J}(\tau) : \tau \in K\} \ge 0.$$

Since K is a compact set in $\mathbb{R}^N$, there exists a subsequence (again denoted by $\{\tau_n\}$) and some $\tau^* \in K$ such that $\tau_n \to \tau^*$ as $n \to \infty$. We denote $\{u[\tau_n]\}$ as the associated sequence of weak solutions of the homogenized problem (2.12). We receive by theorem 2.1 and the fact that $L^\infty \subset L^2$ the uniform boundedness of $\{u[\tau_n]\}$ in $L^2(S; H^1_{\Gamma_D}(\Omega)) \cap H^1(S;[L^2(\Omega)]^3)$. Thus, there exists a subsequence of $\{\tau_n\}$ (again denoted by $\{\tau_n\}$) such that

$$u[\tau_n] \rightharpoonup \tilde{u} \text{ weakly in } L^2(S; H^1_{\Gamma_D}(\Omega)) \cap H^1(S;[L^2(\Omega)]^3). \tag{3.2}$$

In the next step, we prove that $\tilde{u} = u[\tau^*]$. For every τ_n, the function $u[\tau_n]$ is the solution of

$$a(u[\tau_n], v; \tau_n) = F(v; \tau_n)$$

for all $v \in L^2(S; H^1_{\Gamma_D}(\Omega)) \cap H^1(S;[L^2(\Omega)]^3)$ with $v(T) = 0$, where

royalsocietypublishing.org/journal/rspa Proc. R. Soc. A 480: 20240090

$$a : L^2(S; H^1_{\Gamma_D}(\Omega)) \cap H^1(S; [L^2(\Omega)]^3) \times L^2(S; H^1_{\Gamma_D}(\Omega)) \cap H^1(S; [L^2(\Omega)]^3) \to \mathbb{R}$$

is the bilinear form of the left-hand side of (2.12), i.e.

$$\begin{aligned} a(w, v; \hat{\tau}) = &- \int_0^T \int_\Omega \mathcal{M}_Y(\varrho[\hat{\tau}](x, \cdot))\partial_t w(t,x) \cdot \partial_t v(t,x)\, \mathrm{d}x\mathrm{d}t \\ &+ \int_0^T \int_\Omega A^{\mathrm{hom}}[\hat{\tau}](x) e(w)(t,x) e(v)(t,x)\, \mathrm{d}x\mathrm{d}t, \end{aligned}$$

and

$$F : L^2(S; H^1_{\Gamma_D}(\Omega)) \cap H^1(S; [L^2(\Omega)]^3) \to \mathbb{R}$$

is the linear functional of the right-hand side, i.e.

$$\begin{aligned} F(v; \hat{\tau}) = &\int_0^T \int_\Omega f(t,x) \cdot v(t,x)\, \mathrm{d}x\mathrm{d}t + \int_0^T \int_{\Gamma_N} g \cdot v(t,x)\, \mathrm{d}\sigma(x)\mathrm{d}t \\ &+ \int_\Omega \mathcal{M}_Y(\varrho[\hat{\tau}](x, \cdot)) u_1(x) \cdot v(0,x)\, \mathrm{d}x\,. \end{aligned}$$

The index $\hat{\tau}$ emphasizes the dependence of the bilinear form and the linear form on the parameter $\hat{\tau}$ through $A^{\mathrm{hom}}[\hat{\tau}]$ and $\varrho[\hat{\tau}]$. For readability, we omit the arguments (t, x) of the functions.

In the first substep, we show that

$$|a(u[\tau_n], v; \tau_n) - a(\tilde{u}, v; \tau^*)| \to 0 \tag{3.3}$$

for $n \to \infty$. We rewrite the difference and use Hölder's inequality to obtain

$$\begin{aligned} &|a(u[\tau_n], v; \tau_n) - a(\tilde{u}, v; \tau^*)| \\ &\quad \le \|\mathcal{M}_Y(\varrho[\tau_n] - \varrho[\tau^*])\|_{L^\infty(\Omega)} \|\partial_t u[\tau_n]\|_{[L^2(S\times\Omega)]^3} \|\partial_t v\|_{[L^2(S\times\Omega)]^3} \\ &\qquad + \|\mathcal{M}_Y(\varrho[\tau^*])\|_{L^\infty(\Omega)} \left| \int_0^T \int_\Omega \partial_t(u[\tau_n] - \tilde{u}) \cdot \partial_t v\, \mathrm{d}x\mathrm{d}t \right| \\ &\qquad + \|(A^{\mathrm{hom}}[\tau_n] - A^{\mathrm{hom}}[\tau^*]) e(\tilde{u})\|_{[L^2(S\times\Omega)]^{3\times 3}} \|e(v)\|_{[L^2(S\times\Omega)]^{3\times 3}} \\ &\qquad + \left| \int_0^T \int_\Omega \left(\sum_{k,l=1}^3 a^{\mathrm{hom}}_{ijkl}[\tau_n] e_{kl}(v) \right)_{i,j=1,2,3} : (e(u[\tau_n] - \tilde{u}))\, \mathrm{d}x\mathrm{d}t \right|. \end{aligned}$$

For the first summand on the right-hand side, using $0 < \varrho_0, \varrho_1 \in L^\infty(\Omega)$, we receive for a.e. $x \in \Omega$

$$\begin{aligned} &|\mathcal{M}_Y(\varrho[\tau_n](x) - \varrho[\tau^*](x))| \\ &\quad \le \frac{C}{|Y|} (|Y_0[\tau_n] \backslash Y_0[\tau^*] \cup Y_0[\tau^*] \backslash Y_0[\tau_n]| + |Y_1[\tau_n] \backslash Y_1[\tau^*] \cup Y_1[\tau^*] \backslash Y_1[\tau_n]|) \to 0. \end{aligned} \tag{3.4}$$

Since the right-hand side of this inequality is independent of x, we even get the convergence in $L^\infty(\Omega)$. The convergence of the second and the fourth summand is clear. For the third summand, we receive

$$\|(A^{\mathrm{hom}}[\tau_n] - A^{\mathrm{hom}}[\tau^*]) e(\tilde{u})\|_{[L^2(S\times\Omega)]^{3\times 3}} \to 0$$

proceeding precisely as in the proof of [1, theorem 6]. Using the pointwise convergence of $A^{\mathrm{hom}}[\tau_n]$ to $A^{\mathrm{hom}}[\tau^*]$ proven in [1, theorem 7] and the weak convergence (3.2), this shows (3.3).

In the second substep, we prove

$$|F(v, \tau_n) - F(v, \tau^*)| \to 0 \tag{3.5}$$

for $n \to \infty$. Because

$$|F(v; \tau_n) - F(v; \tau^*)| \le C \|\mathcal{M}_Y(\varrho[\tau_n] - \varrho[\tau^*])\|_{L^\infty(\Omega)},$$

(3.5) follows directly from (3.4). So we can conclude from the first and second substeps that

$$a(\tilde{u}, v; \tau^*) = \lim_{n\to\infty} a(u[\tau_n], v; \tau_n) = \lim_{n\to\infty} F(v; \tau_n) = F(v; \tau^*). \tag{3.6}$$

Since $u[\tau_n], \tilde{u} \in L^2(S; H^1_{\Gamma_D}) \cap H^1(S; [L^2(\Omega)]^3)$ we can apply [19, Theorem 10.9] to obtain $u_n, \tilde{u} \in C^0(\bar{S}; [L^2(\Omega)]^3)$. Thus, by using [19, Proposition 10.8]

$$u[\tau_n](t) = \gamma_t(u[\tau_n]), \quad \tilde{u}(t) = \gamma_t(\tilde{u}) \quad \text{for all } t \in \bar{S},$$

where the trace operator γ_t for Bochner spaces is defined in [19, Theorem 10.7]. The definition of the trace operator and the weak convergence of the solutions in $H^1(S; [L^2(\Omega)]^3)$ yield

$$\begin{aligned} u_0(x) = u[\tau_n](0,x) = \gamma_0(u[\tau_n]) &= -\int_0^T u[\tau_n](t)\partial_t\phi(t)\mathrm{d}t - \int_0^T \partial_t u[\tau_n](t)\phi(t)\mathrm{d}t \\ &\to -\int_0^T \tilde{u}(t)\partial_t\phi(t)\mathrm{d}t - \int_0^T \partial_t\tilde{u}(t)\phi(t)\mathrm{d}t = \gamma_0(\tilde{u}) = \tilde{u}(0,x) \end{aligned}$$

for all $\phi \in C_c^\infty([0,T))$ with $\phi(0) = 1$, which shows that

$$\tilde{u}(0,x) = u_0(x).$$

If we summarize all results so far, we obtain that $\tilde{u} = u[\tau^*]$ due to the uniqueness of the solution $u[\tau^*]$ of (2.12). Since the functional $\mathcal{F} : [L^2(S\times\partial\Omega)]^3 \to \mathbb{R}, v \mapsto \|v - u_m\|^2_{L^2(S\times\partial\Omega)}$ is continuous and convex, we obtain by [19, Theorem 13.8] that $\mathcal{F}$ is weakly lower semi-continuous. Thus, we conclude that

$$\mathcal{J}(\tau^*) \le \liminf_{n\to\infty} \mathcal{J}(\tau_n) = \lim_{n\to\infty} \mathcal{J}(\tau_n) = \inf\{\mathcal{J}(\tau) : \tau \in I_\eta\} \le \mathcal{J}(\tau^*),$$

showing that τ^* is a solution of the inverse problem (3.1). ∎

(b) Gâteaux derivative of $\mathcal{J}$

In order to facilitate gradient-based descent methods, we compute the Gâteaux derivative of the functional of the inverse problem (3.1) in this subsection, namely of

$$\mathcal{J}(\tau) = \frac{1}{2}\int_S\int_{\partial\Omega} |\mathcal{L}_\tau(f,g) - u_m|^2 \mathrm{d}\sigma(x)\mathrm{d}t\,.$$

Let $u[\tau]$ and $u[\tau + \varepsilon\hat{\tau}]$ be the weak solutions of (2.12) for given τ and $\tau + \varepsilon\hat{\tau}$, respectively. Taking the difference of both equations, multiplying by $\frac{1}{\varepsilon}$ and passing to the limit yields

$$\begin{aligned} -\int_0^T\int_\Omega \delta\mathcal{M}_Y(\varrho[\tau],\hat{\tau})(x)\partial_t u[\tau]\cdot\partial_t v\,\mathrm{d}x\mathrm{d}t - \int_0^T\int_\Omega \mathcal{M}_Y(\varrho[\tau](x,\cdot))\partial_t(\delta u(\tau,\hat{\tau}))\cdot\partial_t v\,\mathrm{d}x\mathrm{d}t \\ + \int_0^T\int_\Omega \delta A^{\mathrm{hom}}(\tau,\hat{\tau})e(u[\tau])e(v)\,\mathrm{d}x\mathrm{d}t + \int_0^T\int_\Omega A^{\mathrm{hom}}[\tau]e(\delta u(\tau,\hat{\tau}))e(v)\,\mathrm{d}x\mathrm{d}t \\ = \int_\Omega \delta\mathcal{M}_Y(\varrho[\tau],\hat{\tau})(x)u_1(x)\cdot v(0,x)\,\mathrm{d}x\,. \end{aligned} \tag{3.7}$$

To compute $\delta u(\tau,\hat{\tau})$, we require formulas for the Gâteaux derivatives of $\mathcal{M}_Y(\varrho[\tau],\hat{\tau})$ and $A^{\mathrm{hom}}(\tau,\hat{\tau})$. In both cases, we apply the concept of shape derivatives. The following definitions and theorems and further information can be found in [4].

Definition 3.3. *Let Ω_0 be a reference domain, $\Omega = \{x + \theta(x) : x \in \Omega_0\} =: (\mathrm{Id} + \theta)(\Omega_0)$ for some vector field $\theta : \mathbb{R}^3 \to \mathbb{R}^3$. A functional $\mathcal{F} : \Omega \to \mathbb{R}$ is said to be shape differentiable at Ω_0 if the application $\theta \mapsto \mathcal{F}((\mathrm{Id}+\theta)(\Omega_0))$ is Fréchet differentiable at 0 in the Banach space $[W^{1,\infty}(\mathbb{R}^3)]^3$. Then, the following asymptotic expansion holds in the vicinity of 0:*

$$\mathcal{F}((\mathrm{Id}+\theta)(\Omega)) = \mathcal{F}(\Omega) + \mathcal{F}'(\Omega)(\theta) + o(\theta) \quad \text{with} \lim_{\theta \to 0} \frac{|o(\theta)|}{\|\theta\|} = 0,$$

where $\mathcal{F}'(\Omega)$ is a continuous linear form on $[W^{1,\infty}(\mathbb{R}^3)]^3$.

We can also define directional derivatives as in the standard differentiation of functions.

Definition 3.4. *The directional derivative of a functional $\mathcal{F}: \Omega \to \mathbb{R}$ at Ω in the direction $\theta \in [W^{1,\infty}(\mathbb{R}^3)]^3$ (if it exists) is defined by*

$$\mathcal{F}'(\Omega)(\theta) = \lim_{\delta \to 0} \frac{\mathcal{F}((\mathrm{Id}+\delta\theta)\Omega) - \mathcal{F}(\Omega)}{\delta}.$$

The following two theorems give the shape derivative for functionals, where the integrand does not depend on the domain.

Theorem 3.3. *Let $\Omega_0 \subset \mathbb{R}^3$ a smooth bounded open set. If $f \in W^{1,1}(\mathbb{R}^3)$ and $\mathcal{F}: \mathbb{C}(\Omega_0) \to \mathbb{R}$ is defined by $\mathcal{F}(\Omega) = \int_\Omega f(x)\,\mathrm{d}x$, where $\mathbb{C}(\Omega_0) := \{\Omega = (\mathrm{Id}+\theta)(\Omega_0)$ with $\theta \in [W^{1,\infty}(\mathbb{R}^3)]^3\}$, then $\mathcal{F}$ is differentiable at Ω_0 and*

$$\mathcal{F}'(\Omega_0)(\theta) = \int_{\Omega_0} \mathrm{div}(\theta(x) f(x))\,\mathrm{d}x = \int_{\partial\Omega_0} \theta(x)\cdot n(x) f(x)\,\mathrm{d}\sigma(x)$$

for all $\theta \in [W^{1,\infty}(\mathbb{R}^3)]^3$.

The theorem still holds if Ω_0 is regular enough to apply the transformation formula and Gauß's theorem.

Theorem 3.4. *Let $\Omega_0 \subset \mathbb{R}^3$ be a smooth bounded open set. If $f \in W^{2,1}(\mathbb{R}^3)$ and $\mathcal{F}: \mathbb{C}(\Omega_0) \to \mathbb{R}$ is defined by $\mathcal{F}(\Omega) = \int_{\partial\Omega} f(x)\,\mathrm{d}\sigma(x)$, where $\mathbb{C}(\Omega_0) := \{\Omega = (\mathrm{Id}+\theta)(\Omega_0)$ with $\theta \in [W^{1,\infty}(\mathbb{R}^3)]^3\}$, then $\mathcal{F}$ is differentiable at Ω_0 and for all $\theta \in [W^{1,\infty}(\mathbb{R}^3)]^3$*

$$\mathcal{F}'(\Omega_0)(\theta) = \int_{\partial\Omega_0} \nabla f\cdot\theta + f(\mathrm{div}\,\theta - \nabla\theta n\cdot n)\,\mathrm{d}\sigma(x) = \int_{\partial\Omega_0}\left(\frac{\partial f}{\partial n} + Hf\right)\theta\cdot n\,\mathrm{d}\sigma(x),$$

where $H = \mathrm{div}\, n$ is the mean curvature of $\partial\Omega_0$.

We present the main ideas for deriving the Gâteaux derivative of A^{hom}, more details can be found in [1]. We use the Lagrangian method of Céa following the idea of Allaire *et al*. outlined in [5]. In a first step, we consider the tensor A^{hom} as a function of the domain Y_0, i.e.

$$\mathfrak{F}^x_{ijkl}(Y_0) := \frac{1}{|Y|}\int_Y B[Y_0](x,y)e_{ij}(e_{kl} - e(w_{kl})(x,y))\,\mathrm{d}y$$

for every $x \in \Omega$ with $B[Y_0](x,y) := A^0(x)\chi_{Y_0}(y) + A^1(x)(1-\chi_{Y_0}(y))$ and $w_{kl} \in [L^\infty(\Omega, H^1_{\mathrm{per}}(Y))]^3$ the weak solution of

$$\begin{cases} -\mathrm{div}_y(B[Y_0](x,\,\cdot\,)(e_y(w_{kl}) - e_{kl})) = 0 & \text{in } Y, \\ \mathcal{M}_Y(w_{kl}) = 0. \end{cases} \tag{3.8}$$

Since w_{kl} also depend on the domain Y_0 we cannot apply the standard shape-derivative results directly. So, we rewrite the cell problem as a transmission problem to define a Lagrangian function $\mathfrak{L}^x_{ijkl}$ which coincides with $\mathfrak{F}^x_{ijkl}$ in some points. The main advantage is that we can apply the standard shape-derivative results for the shape derivative of $\mathfrak{L}^x_{ijkl}$. For readability, we omit the index y in the divergence $\mathrm{div}_y(\,\cdot\,)$ and the symmetric gradient $e_y(\,\cdot\,)$.

So, for a.e. $x \in \Omega$, find

$$(w^{x,0}_{kl}, w^{x,1}_{kl}) \in V := \{(u^0,u^1) \in [H^1(Y_0)]^3 \times [H^1(Y_1)]^3 : u^1 \text{ is Y-periodic, } \mathcal{M}_Y(u^1\chi_{Y_1} + u^0\chi_{Y_0}) = 0\}$$

such that

$$\begin{cases} -\operatorname{div}(A_x^\alpha(e(w_{kl}^{x,\alpha}) - e_{kl})) = 0 & \text{in } Y_\alpha, \\ w_{kl}^{x,1} = w_{kl}^{x,0} & \text{on } \Sigma_Y, \\ A_x^1(e(w_{kl}^{x,1}) - e_{kl}))n^1 + A_x^0(e(w_{kl}^{x,0}) - e_{kl}))n^0 = 0 & \text{on } \Sigma_Y, \end{cases} \tag{3.9}$$

for $\alpha \in \{0,1\}$, where $A_x^0 := A^0(x)$, $A_x^1 := A^1(x)$ and $n = n^0 = -n^1$ is the outward unit normal vector of the interface $\Sigma_Y = \partial Y_0$ with direction from Y_0 to Y_1. Clearly, the transmission problem is equivalent to (3.8).

We also define the adjoint transmission problem: Find $(p^0, p^1) \in V$ such that

$$\begin{cases} -\operatorname{div}(A_x^\alpha(e(p^\alpha) + e_{ij})) = 0 & \text{in } Y_\alpha, \\ p^1 = p^0 & \text{on } \Sigma_Y, \\ A_x^1(e(p^1) + e_{ij}))n^1 + A_x^0(e(p^0) + e_{ij}))n^0 = 0 & \text{on } \Sigma_Y \end{cases} \tag{3.10}$$

for $\alpha \in \{0,1\}$, which is equivalent to

$$\begin{cases} -\operatorname{div}(B[Y_0](x, \cdot)(e(p) + e_{ij})) = 0 & \text{in } Y, \\ \mathcal{M}_Y(p) = 0. \end{cases} \tag{3.11}$$

Obviously, the function $-w_{ij}^x := -w_{ij}(x, \cdot)$ with w_{ij} the solution of (3.8) for $k = i, l = j$ is a solution of (3.11).

Introducing the Lagrangian function

$$\begin{aligned} \mathfrak{L}_{ijkl}^x(v^0, v^1, q^0, q^1, Y_0) := \frac{1}{|Y|}\Bigg(& -\int_{Y_0} A_x^0(e(q^0) + e_{ij})(e(v^0) - e_{kl})\,\mathrm{d}y \\ & - \int_{Y_1} A_x^1(e(q^1) + e_{ij})(e(v^1) - e_{kl})\,\mathrm{d}y \\ & - \frac{1}{2}\int_{\Sigma_Y} (A_x^1(e(v^1) - e_{kl}) + A_x^0(e(v^0) - e_{kl}))n \cdot (q^1 - q^0)\,\mathrm{d}\sigma(y) \\ & - \frac{1}{2}\int_{\Sigma_Y} (A_x^1(e(q^1) + e_{ij}) + A_x^0(e(q^0) + e_{ij}))n \cdot (v^1 - v^0)\,\mathrm{d}\sigma(y)\Bigg) \end{aligned}$$

for $v^0, v^1, q^0, q^1 \in [H^1_{\mathrm{per},0}(Y)]^3$, where q^1, q^0 play the role of Lagrange multipliers, we obtain some conditions for optimal points.

Theorem 3.5. *The solutions* (u^0, u^1) *of the transmission problem* (3.9) *and* (p^0, p^1) *of the adjoint transmission problem* (3.11) *satisfy the optimality conditions*

$$0 = \frac{\partial \mathfrak{L}_{ijkl}^x}{\partial q^1}(u^0, u^1, q^0, q^1, Y_0)(\phi) = \frac{\partial \mathfrak{L}_{ijkl}^x}{\partial q^0}(u^0, u^1, q^0, q^1, Y_0)(\phi) \tag{3.12}$$

for all $q^0, q^1, \phi \in [H^1_{\mathrm{per},0}(Y)]^3$ *and*

$$0 = \frac{\partial \mathfrak{L}_{ijkl}^x}{\partial v^1}(v^0, v^1, p^0, p^1, Y_0)(\phi) = \frac{\partial \mathfrak{L}_{ijkl}^x}{\partial v^0}(v^0, v^1, p^0, p^1, Y_0)(\phi) \tag{3.13}$$

for all $v^0, v^1, \phi \in [H^1_{\mathrm{per},0}(Y)]^3$. *Therefore, the solutions* $w_{kl}^x := w_{kl}(x, \cdot)$ *fulfil the condition* (3.12) *for* $(u^0, u^1) = (w_{kl}^x, w_{kl}^x)$ *and the solutions* $w_{ij}^x := w_{ij}(x, \cdot)$ *of* (3.8) *the condition* (3.13) *for* $(p^0, p^1) = (-w_{ij}^x, -w_{ij}^x)$.

Proof. Let $q^0, q^1, \phi \in [H^1_{\mathrm{per},0}(Y)]^3$. We compute the directional derivatives by using integration by parts

$$\frac{\partial \mathfrak{L}^x_{ijkl}}{\partial q^\alpha}(v^0, v^1, q^0, q^1, Y_0)(\phi) = \frac{1}{|Y|}\Big(\int_{Y_\alpha} \operatorname{div}(A^\alpha_x(e(v^\alpha) - e_{kl}))\phi \,\mathrm{d}y + \frac{1}{2}\int_{\Sigma_Y} (A^1_x(e(v^1) - e_{kl}) - A^0_x(e(v^0) - e_{kl}))n \cdot \phi \,\mathrm{d}\sigma(y) - \frac{1}{2}\int_{\Sigma_Y} A^\alpha_x e(\phi)n \cdot (v^1 - v^0)\,\mathrm{d}\sigma(y)\Big)$$

for $\alpha \in \{0,1\}$. So (3.12) and, due to the equivalence of the problems (3.8) and (3.9), the statement of the theorem for $(u^0, u^1) = (w^x_{kl}, w^x_{kl})$ follow directly. The proof for (p^0, p^1) resp. $(-w^x_{ij}, -w^x_{ij})$ follows analogously. ∎

Although the weak solution w_{kl} of the cell problem (3.8) is not shape differentiable, the restricted functions $w^{x,0}_{kl}$ and $w^{x,1}_{kl}$ are shape differentiable.

Theorem 3.6. *The solution $w^{x,\alpha}_{kl}$, $\alpha \in \{0,1\}$, of (3.9) is shape differentiable for a.e. $x \in \Omega$ and $\theta \in [W^{1,\infty}_0(Y)]^3$.*

Proof. The lemma can be shown as in the proof of [22, theorem 5.3.2] by the implicit function theorem. ∎

We are now able to prove that $\mathfrak{L}^x_{ijkl}$ coincides with $\mathfrak{F}^x_{ijkl}(Y_0)$ in the optimal point $(w^{x,0}_{kl}, w^{x,1}_{kl}, -w^{x,0}_{ij}, -w^{x,1}_{ij}, Y_0)$, whereby we write $w^{x,\alpha}_{kl}$, $\alpha \in \{0,1\}$, instead of w^x_{kl} to emphasize which problem w^x_{kl} solves and that only the values in Y_α are relevant for the calculation of $\mathfrak{L}^x_{ijkl}$.

Theorem 3.7. *The shape derivative of the objective function $\mathfrak{F}^x_{ijkl}(Y_0)$ exists and is given by*

$$(\mathfrak{F}^x_{ijkl})'(Y_0)(\theta) = \frac{\partial \mathfrak{L}^x_{ijkl}}{\partial Y_0}(w^{x,0}_{kl}, w^{x,1}_{kl}, -w^{x,0}_{ij}, -w^{x,1}_{ij}, Y_0)(\theta)$$

for all $\theta \in [W^{1,\infty}_0(Y)]^3$.

Proof. Using the solution properties of $w^{x,1}_{kl}$ and $w^{x,0}_{kl}$, there holds for all $q^0, q^1 \in [H^1_{\mathrm{per},0}(Y)]^3$

$$\begin{aligned}\mathfrak{L}^x_{ijkl}(w^{x,0}_{kl}, w^{x,1}_{kl}, q^0, q^1, Y_0) &= \mathfrak{F}^x_{ijkl}(Y_0) + \frac{1}{|Y|}\Big(-\int_{Y_0} A^0_x(e(w^{x,0}_{kl}) - e_{kl})e(q^0)\,\mathrm{d}y - \int_{Y_1} A^1_x(e(w^{x,1}_{kl}) - e_{kl})e(q^1)\,\mathrm{d}y \\ &\quad + \int_{\Sigma_Y} (A^1_x(e(w^{x,1}_{kl}) - e_{kl})n^1 \cdot q^1 + A^0_x(e(w^{x,0}_{kl}) - e_{kl}))n^0 \cdot q^0 \,\mathrm{d}\sigma(y)\Big) = \mathfrak{F}^x_{ijkl}(Y_0)\,.\end{aligned}$$

We differentiate this identity with respect to shape,

$$(\mathfrak{F}^x_{ijkl})'(Y_0)(\theta) = \frac{\partial \mathfrak{L}^x_{ijkl}}{\partial Y_0}(w^{x,0}_{kl}, w^{x,1}_{kl}, q^0, q^1, Y_0)(\theta) + \sum_{\alpha=0}^{1} \frac{\partial \mathfrak{L}^x_{ijkl}}{\partial v^\alpha}(w^{x,0}_{kl}, w^{x,1}_{kl}, q^0, q^1, Y_0)\frac{\partial w^{x,\alpha}_{kl}}{\partial Y_0}(\theta)\,.$$

Choosing $q^0 = -w^{x,0}_{ij}$ and $q^1 = -w^{x,1}_{ij}$, the last two terms disappear by theorem 3.5. ∎

We are now able to apply the standard shape-derivative results to compute the shape derivative of the Lagrangian $\mathfrak{L}^x_{ijkl}$ since v^0, v^1, q^0, q^0 do not depend on the structure of Y_0.

Theorem 3.8. *The shape derivative of $\mathfrak{L}^x_{ijkl}$ is of the form*

royalsocietypublishing.org/journal/rspa Proc. R. Soc. A 480: 20240090

$$\begin{aligned}
&\frac{\partial \mathfrak{L}^x_{ijkl}}{\partial Y_0}(w^{x,0}_{kl}, w^{x,1}_{kl}, -w^{x,0}_{ij}, -w^{x,1}_{ij}, Y_0)(\theta \\
&\quad = \frac{1}{|Y|}\Bigg(\int_{\Sigma_Y} A^0_x(e(w^{x,0}_{kl}) - e_{kl})(e(w^{x,0}_{ij}) - e_{ij})\theta \cdot n \, \mathrm{d}\sigma(y) \\
&\qquad - \int_{\Sigma_Y} A^1_x(e(w^{x,1}_{kl}) - e_{kl})(e(w^{x,1}_{ij}) - e_{ij})\theta \cdot n \, \mathrm{d}\sigma(y) \\
&\qquad + \int_{\Sigma_Y} A_x(e(w^x_{kl}) - e_{kl})n \cdot \frac{\partial(w^{x,1}_{ij} - w^{x,0}_{ij})}{\partial n}\theta \cdot n \, \mathrm{d}\sigma(y) \\
&\qquad + \int_{\Sigma_Y} A_x(e(w^x_{ij}) - e_{ij})n \cdot \frac{\partial(w^{x,1}_{kl} - w^{x,0}_{kl})}{\partial n}\theta \cdot n \, \mathrm{d}\sigma(y)\Bigg),
\end{aligned} \tag{3.14}$$

where we denote by $A_x(e(w^x_{kl}) - e_{kl})n$ *and* $A_x(e(w^x_{ij}) - e_{ij})n$ *the continuous quantities through the interface.*

Proof. We apply theorems 3.3 and 3.4 to $\mathfrak{L}^x_{ijkl}$ and use the fact that the terms involving H vanish on Σ_Y, since $w^{x,1}_{kl} = w^{x,0}_{kl}$ and $w^{x,1}_{ij} = w^{x,0}_{ij}$ on Σ_Y, and $A^1_x(e(w^{x,1}_{kl}) - e_{kl})n = A^0_x(e(w^{x,0}_{kl}) - e_{kl})n$ on Σ_Y. ∎

Remark 3.1. *Formula* (3.14) *holds for general elasticity tensors* A^0_x *and* A^1_x. *It can be simplified for materials defined by less material parameters. For example, if we assume isotropic materials the shape derivative* $\partial \mathfrak{L}^x_{ijkl}/\partial Y_0$ *can be rewritten in a simpler computational formula involving the materials' Lamé parameters* λ_x *and* μ_x, *that is*

$$\begin{aligned}
&\frac{\partial \mathfrak{L}^x_{ijkl}}{\partial Y_0}(w^{x,0}_{kl}, w^{x,1}_{kl}, -w^{x,0}_{ij}, -w^{x,1}_{ij}, Y_0)(\theta) \\
&\quad = \int_{\Sigma_Y}\Bigg(-[2\mu_x](e(w^x_{kl}) - e_{kl})_{tt}(e(w^x_{ij}) - e_{ij})_{tt} \\
&\qquad - \left[\frac{2\mu_x\lambda_x}{2\mu_x + \lambda_x}\right]\mathrm{tr}(e(w^x_{kl}) - e_{kl})_{tt}\mathrm{tr}(e(w^x_{ij}) - e_{ij})_{tt} \\
&\qquad + \left[\frac{1}{\mu_x}\right](A_x(e(w^x_{kl}) - e_{kl}))_{tn}(A_x(e(w^x_{ij}) - e_{ij}))_{tn} \\
&\qquad + \left[\frac{1}{2\mu_x + \lambda_x}\right](A_x(e(w^x_{kl}) - e_{kl}))_{nn}(A_x(e(w^x_{ij}) - e_{ij}))_{nn} \\
&\qquad - \left[\frac{\lambda_x}{2\mu_x + \lambda_x}\right](A_x(e(w^x_{kl}) - e_{kl}))_{nn}\mathrm{tr}(e(w^x_{ij}) - e_{ij})_{tt} \\
&\qquad - \left[\frac{\lambda_x}{2\mu_x + \lambda_x}\right](A_x(e(w^x_{ij}) - e_{ij}))_{nn}\mathrm{tr}(e(w^x_{kl}) - e_{kl})_{tt}\Bigg)\theta \cdot n \, \mathrm{d}\sigma(y)
\end{aligned} \tag{3.15}$$

for all $\theta \in [W^{1,\infty}_0(Y)]^3$ *(see [1, theorem 9]).*

In order to be able to compute the shape derivative explicitly, we now assume that there exist $\Theta_\alpha \in [W^{1,\infty}_0(Y)]^3$, $\alpha \in \{1, \ldots, N\}$, which satisfy

$$(\mathrm{Id} + \delta\tau_1\Theta_1 + \ldots + \delta\tau_N\Theta_N)(Y[\tau]) = Y[\tau_1 + \delta\tau_1, \ldots, \tau_N + \delta\tau_N], \tag{3.16}$$

i.e. the structural assumption is maintained. So in this case, by theorem 3.7,

$$\frac{\partial a^{\mathrm{hom}}_{ijkl}}{\partial \tau_\alpha}[\tau](x) = (\mathfrak{F}^x_{ijkl})'(\Theta_\alpha) = \frac{\partial \mathfrak{L}^x_{ijkl}}{\partial Y_0}(\Theta_\alpha).$$

Using this result, the Gâteaux derivative $\delta A^{\mathrm{hom}}(\tau, \hat{\tau}) = (\delta a^{\mathrm{hom}}_{ijkl}(\tau, \hat{\tau}))_{1 \le i,j,k,l \le 3}$,

$$\delta a^{\mathrm{hom}}_{ijkl}(\tau, \hat{\tau})(x) = \sum_{\alpha=1}^{N} \frac{\partial a^{\mathrm{hom}}_{ijkl}}{\partial \tau_\alpha}[\tau](x)\hat{\tau}_\alpha \in L^\infty(\Omega),$$

can be computed by (3.14) or, in the case of isotropic materials, by (3.15).

Remark 3.2. *In the case that $Y_0[\tau]$ is an open ellipsoid with $\tau = (\tau_1, \tau_2, \tau_3) \in [\kappa, l_1 - \kappa] \times [\kappa, l_2 - \kappa] \times [\kappa, l_3 - \kappa] =: I_\kappa$ for some small κ, where τ_1, τ_2, and τ_3 are the lengths of the axes, and $Y_0[\tau]$ is centred in the middle of the cuboid Y with axes in direction of the standard unit vectors, explicit formulas for $\Theta_\alpha \in [W_0^{1,\infty}(Y)]^3$, $\alpha \in \{1,2,3\}$, are given in [1, (24)–(26)], which satisfy (3.16).*

It remains to compute the Gâteaux derivative of $\mathcal{M}_Y(\varrho[\tau])$. We define

$$\mathcal{F}(Y) = \int_{Y_0} \varrho_0(x)\,\mathrm{d}y + \int_{Y_1} \varrho_1(x)\,\mathrm{d}y =: \mathcal{F}_1(Y_0) + \mathcal{F}_1(Y_1)$$

for a.e. $x \in \Omega$ and compute the directional derivative

$$\begin{aligned}\mathcal{F}'(Y)(\theta) &= \lim_{\delta \to 0} \frac{\mathcal{F}((\mathrm{Id} + \delta\theta)(Y)) - \mathcal{F}(Y)}{\delta} \\ &= \lim_{\delta \to 0} \frac{\mathcal{F}_1((\mathrm{Id} + \delta\theta)(Y_0)) + \mathcal{F}_2((\mathrm{Id} + \delta\theta)(Y_1)) - \mathcal{F}_1(Y_0) - \mathcal{F}_2(Y_1)}{\delta} \\ &= \mathcal{F}_1'(Y_0)(\theta) + \mathcal{F}_2'(Y_1)(\theta)\end{aligned}$$

for all $\theta \in [W^{1,\infty}(\mathbb{R}^3)]^3$. Owing to theorem 3.3, the last two terms exist and can be rewritten as

$$\mathcal{F}'(Y)(\theta) = \int_{\partial Y_0} \varrho_0(x)\theta \cdot n\,\mathrm{d}\sigma(y) + \int_{\partial Y} \varrho_1 \theta \cdot n\,\mathrm{d}\sigma(y) + \int_{\partial Y_0} \varrho_1(x)\theta \cdot (-n)\,\mathrm{d}\sigma(y).$$

Since $\frac{1}{|Y|}\mathcal{F}(Y[\tau]) = \mathcal{M}_Y(\varrho[\tau])$ and the integrals $\int_{\partial Y} \varrho_1(x)\Theta_\alpha \cdot n\,\mathrm{d}\sigma(y)$ vanish due to the definition of Θ_α for $\alpha \in \{1, \ldots, N\}$, we obtain

$$\begin{aligned}\delta\mathcal{M}_Y(\varrho[\tau], \hat{\tau})(x) &= \sum_{\alpha=1}^{N} \frac{1}{|Y|}\mathcal{F}'(Y[\tau])(\Theta_\alpha)\hat{\tau}_\alpha \\ &= \frac{1}{|Y|}\int_{\partial Y_0[\tau]} (\varrho_0(x) - \varrho_1(x))(\hat{\tau}_1\Theta_1 + \ldots + \hat{\tau}_N\Theta_N) \cdot n\,\mathrm{d}\sigma(y)\,.\end{aligned}$$

Finally having formulas for the Gâteaux derivatives of $\mathcal{M}_Y(\varrho[\tau], \hat{\tau})$ and $A^{\mathrm{hom}}(\tau, \hat{\tau})$ at hand, we can return to (3.7) to compute $\delta u(\tau, \hat{\tau})$. In the case that ρ_0 and ρ_1 are independent of x, we get that $\partial_t(\delta\mathcal{M}_Y(\varrho[\tau], \hat{\tau})\partial_t u[\tau]) \in L^2(S, (H^1_{\Gamma_D}(\Omega))^*)$. So we can apply [23, Satz 1.1] to get the existence and uniqueness of the solution $\delta u(\tau, \hat{\tau}) \in L^2(S; H^1_{\Gamma_D}(\Omega)) \cap H^1(S; [L^2(\Omega)]^3)$ of (3.7) with initial condition $\delta u(\tau, \hat{\tau})(0, x) = 0$. More general ρ_0 and ρ_1 are possible as long as $\partial_t(\delta\mathcal{M}_Y(\varrho[\tau], \hat{\tau})\partial_t u[\tau]) \in L^2(S, (H^1_{\Gamma_D}(\Omega))^*)$. We rewrite the problem: find functions $\partial u/\partial\tau_\alpha$, $\alpha \in \{1, \ldots, N\}$, such that

$$\begin{aligned}&-\int_0^T \int_\Omega \mathcal{M}_Y(\varrho[\tau](x, \cdot))\partial_t\left(\frac{\partial u}{\partial \tau_\alpha}\right) \cdot \partial_t v\,\mathrm{d}x\mathrm{d}t + \int_0^T \int_\Omega A^{\mathrm{hom}}[\tau]e\left(\frac{\partial u}{\partial \tau_\alpha}\right)e(v)\,\mathrm{d}x\mathrm{d}t \\ &= \int_\Omega \frac{\partial \mathcal{M}_Y}{\partial \tau_\alpha}(\varrho[\tau])(x)u_1(x) \cdot v(0, x)\,\mathrm{d}x + \int_0^T \int_\Omega \frac{\partial \mathcal{M}_Y}{\partial \tau_\alpha}(\varrho[\tau])(x)\partial_t u[\tau] \cdot \partial_t v\,\mathrm{d}x\mathrm{d}t \\ &\quad - \int_0^T \int_\Omega \frac{\partial A^{\mathrm{hom}}}{\partial \tau_\alpha}[\tau]e(u[\tau])e(v)\,\mathrm{d}x\mathrm{d}t,\end{aligned} \tag{3.17}$$

where

$$\frac{\partial \mathcal{M}_Y}{\partial \tau_\alpha}(\varrho[\tau])(x) = \frac{1}{|Y|}\int_{\partial Y_0[\tau]} (\varrho_0(x) - \varrho_1(x))\Theta_\alpha(y) \cdot n\,\mathrm{d}\sigma(y)\,.$$

Then, due to uniqueness

$$\nabla u[\tau] \cdot \hat{\tau} = \sum_{\alpha=1}^{N} \frac{\partial u}{\partial \tau_\alpha}\hat{\tau}_\alpha = \delta u(\tau, \hat{\tau}). \tag{3.18}$$

Using (3.18), we can finally compute the Gâteaux derivative of the objective functional as

$$\begin{aligned}\delta\mathcal{J}(\tau,\widehat{\tau}) &= \lim_{\varepsilon\to 0}\frac{1}{2\varepsilon}\int_S\int_{\partial\Omega}|u[\tau+\varepsilon\widetilde{\tau}]-u_{\mathrm{m}}|^2-|u[\tau]-u_{\mathrm{m}}|^2\,\mathrm{d}\sigma(x)\mathrm{d}t\\ &= \int_S\int_{\partial\Omega}(u[\tau]-u_{\mathrm{m}})\delta u(\tau,\widehat{\tau})\,\mathrm{d}\sigma(x)\mathrm{d}t\\ &= \int_S\int_{\partial\Omega}(u[\tau]-u_{\mathrm{m}})\nabla u[\tau]\mathrm{d}\sigma(x)\mathrm{d}t\cdot\widehat{\tau}=:\nabla\mathcal{J}(\tau)\cdot\widehat{\tau},\end{aligned}\tag{3.19}$$

where the components of $\nabla u[\tau]$ are the solution of (3.17) for $\alpha = 1,\ldots,N$.

4. Simulation results

The formulas derived in §3b allow us to run numerical simulations showcasing the functioning of the method. As a concrete example, we consider a generic non-destructive testing problem for a beam occupying the volume $[0,60]\times[0,30]\times[0,30]$ [mm^3] (as depicted in figure 1) made up of concrete ($\varrho_1 = 2300$ [kg/m^3], $\lambda_1 = 5.55$ [GPa], $\mu_1 = 8.33$ [GPa]) and polyvinyl chloride (PVC) ($\varrho_0 = 1400$ [kg/m^3], $\lambda_0 = 1.15$ [GPa], $\mu_0 = 0.36$ [GPa]), where the ellipsoidal PVC inclusions are arranged periodically on the microscale.

Owing to the different scales, we non-dimensionalize the cell problem, i.e. we consider the (non-dimensional) reference cell of sidelengths $2\times1\times1$ with the PVC ellipsoid centred in the middle of the cuboid with axis lengths $(\tau_1,\tau_2,\tau_3)\in K = [0.12,1.88]\times[0.12,0.88]^2$ and the rest of the cell filled up with concrete (see figure 2).

For the non-destructive test, we assume that the beam is fixed on one of the small lateral faces of the cuboid (f_{left} in figure 1). Furthermore, we assume no volume force but we apply a normal boundary load for seven seconds given by $b\cdot\exp(-1/2((t-2)/0.2)^2)$, $b\in\mathbb{R}^3$ and $t\in[0,7]$ [s]($=S$), applied on two faces of the cuboid, such that $b = (0,0,-20)$ at the upper face (f_{up} in figure 1) and $b = (0,-10,0)$ on the back lateral face (f_{back} in figure 1) and $b = (0,0,0)$ on all other faces. Already knowing that the PVC inclusions are of ellipsoidal structure, we want to solve the inverse problem to obtain their exact dimension, i.e. the (vector-valued) parameter τ.

(a) Specification of the different numerical experiments

In what follows, we consider five different numerical experiments. In the first one, the parameter-identification problem is of the form

$$\operatorname*{argmin}_{\tau\in K}\mathcal{J}_1(\tau) := \operatorname*{argmin}_{\tau\in K}\frac{1}{2|\partial\Omega|^2}\int_S\int_{\partial\Omega}|u[\tau]-u_{\mathrm{m}}|^2\,\mathrm{d}\sigma(x)\mathrm{d}t,\tag{4.1}$$

where u_{m} is the deformation of the beam computed for the target value $\tau^{\mathrm{target}} = (1.5, 0.6, 0.4)$ and $u[\tau]$ is the deformation for given τ. The scaling with the constant $\frac{1}{|\partial\Omega|^2}$ has no impact on the derived formula (3.19) apart from a scaling factor. The second numerical experiment is as the first one except that only measured data on part of the boundary of the sample Ω is available, i.e. the parameter-identification problem is of the form

$$\operatorname*{argmin}_{\tau\in K}\mathcal{J}_2(\tau) := \operatorname*{argmin}_{\tau\in K}\frac{1}{2|f_{\mathrm{up}}\cup f_{\mathrm{back}}|^2}\int_S\int_{f_{\mathrm{up}}\cup f_{\mathrm{back}}}|u[\tau]-u_{\mathrm{m}}|^2\,\mathrm{d}\sigma(x)\mathrm{d}t\,.\tag{4.2}$$

The analysis for this slightly modified target functional follows analogously as for the target functional with full boundary displacement information. The third and fourth cases are as the second one, except that noisy boundary data are used, i.e. u_{m} is replaced by $\widetilde{u}_{\mathrm{m}}$ given by the (exact) measured data plus noise, $\widetilde{u}_{\mathrm{m}} = (1+r)u_{\mathrm{m}}$ with a Gaussian random function r of mean value zero and standard deviation 0.03 (third experiment), respectively, 0.09 (fourth experiment). To test the inverse method for the case of inexactly known material parameters

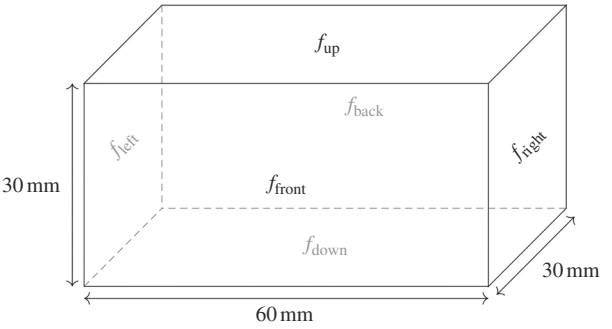

Figure 1. Macroscopic beam with faces labelled f_{front}, f_{back}, f_{up}, f_{down}, f_{left} and f_{right}.

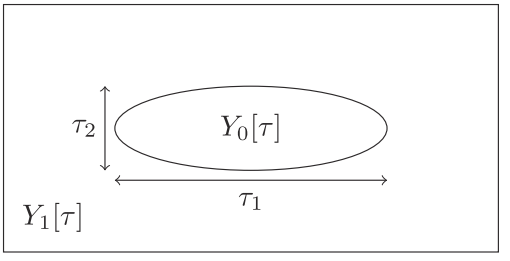

Figure 2. Slice of the reference cell Y, i.e. $[0,2] \times [0,1] \times \{0.5\}$.

as well, the fifth experiment is as the first one again but with noisy data of the Lamé parameters (representing material variations) and measured data, i.e. u_m is replaced by $\tilde{\tilde{u}}_m$ with $\tilde{\tilde{u}}_m = (1 + r)\hat{u}_m$ with a Gaussian random function r of mean value zero and standard deviation 0.03, where $\hat{u}_m$ is the deformation of the beam computed for the target value $\tilde{\tau}^{target} = (1 + r)\tau^{target}$ with a Gaussian random function r of mean value zero and standard deviation 0.03.

The method devised in §3 is implemented in MATLAB® (version R2020a) and COMSOL LiveLink™ for MATLAB®. The main computation is done with the finite element simulation software COMSOL Multiphysics® [24], i.e. we solve for every τ numerically the cell problem (2.13), the homogenized problem (2.12) and the problem for the Gâteaux derivative of u (3.17), whereby quadratic Lagrange finite elements are used. With the solution of these problems, we are able to determine the target functional (4.1) (or (4.2)) and its Gâteaux derivative (3.19). These values are needed to apply the gradient method `fmincon` in MATLAB®, which solves the minimization problem (4.1) (or (4.2)).

We start with a value in the lower left corner of K as an initial guess, i.e. $\tau = (0.12, 0.12, 0.12)$. In all five numerical experiments, we plot in one figure panel the values of τ_1, τ_2 and τ_3 in every iteration step and the target value $\tau^{target} = (\tau_1^{target}, \tau_2^{target}, \tau_3^{target}) = (1.5, 0.6, 0.4)$ as horizontal lines and in the other panel the values of the respective target functional $\mathcal{J}_i$, $i = 1,2$, in each iteration step. The final iteration step always corresponds to the algorithm having terminated because the relative changes in all elements of τ is less than the prescribed step tolerance of 10^{-6} (the default value of `fmincon`).

(b) Discussion of the results

In the first numerical experiment as described above, the algorithm terminates after 49 steps. We obtain as an optimal solution $\tau = (1.492, 0.602, 0.401)$ (see figure 3). This first example with (numerically) exact data confirms the functioning of the method and implementation.

In the second simulation, where the measured data is known only on a part of the boundary, the algorithm terminates after 37 steps. We obtain as an optimal solution $\tau = (1.493, 0.602, 0.402)$

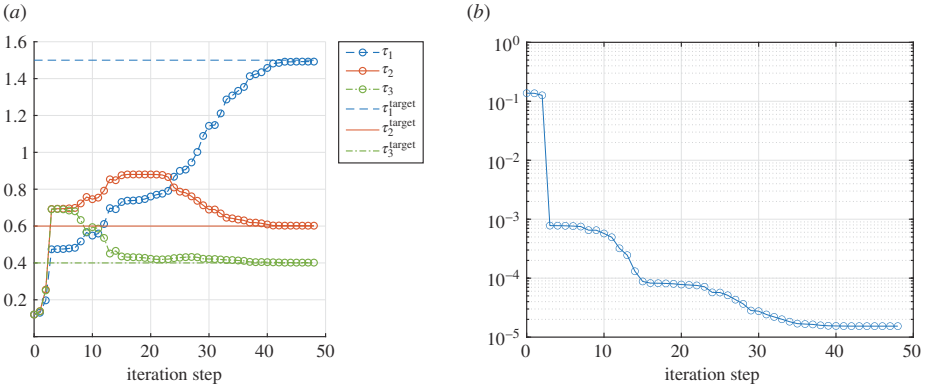

Figure 3. (*a*) Values of $\tau = (\tau_1, \tau_2, \tau_3)$ in each iteration step as well as target values (horizontal lines) in the first numerical experiment. (*b*) Corresponding values of the target functional in each iteration step plotted on a semi-logarithmic scale.

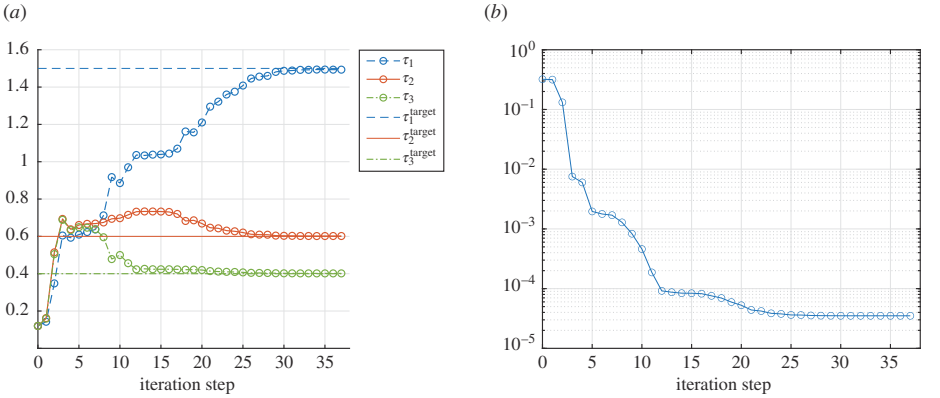

Figure 4. (*a*) Values of $\tau = (\tau_1, \tau_2, \tau_3)$ in each iteration step as well as target values (horizontal lines) in the second numerical experiment. (*b*) Corresponding values of the target functional in each iteration step plotted on a semi-logarithmic scale.

(see figure 4). Therefore, in this case with reduced information (but numerically exact data), we obtain virtually the same results within fewer iterations. This seems to be related to the fact that the algorithm starts out a bit more gradual which avoids the stronger overshooting of the values of τ_2 and τ_3 in iteration three compared with the first experiment.

In the third simulation, where 3% noise is added to the measured data, the algorithm terminates after 35 steps. We obtain as an optimal solution $\tau = (1.456, 0.612, 0.409)$ (see figure 5). While a small error between the elements of the computed solution τ and the target values remains, this is not surprising as only noisy data, as is typically available in practice, was available to the inverse method. As the error is only small, this confirms the usefulness of the method in practice. To push the method further, 9% noise is added to the measured data for the fourth simulation, where the algorithm terminates similarly fast after 36 steps. We obtain as an optimal solution $\tau = (1.582, 0.583, 0.392)$ (see figure 6), which is still not too far off considering the stronger noise in the data available to the inverse method.

In the fifth simulation, where 3% noise is added to the Lamé parameters (inexactly known material parameters) and measured data (measurement imperfection), the algorithm terminates after 48 steps, similar to the first simulation (in which also the whole boundary was used). We obtain as an optimal solution $\tau = (1.764, 0.549, 0.367)$ (see figure 7), which still recovers the general aspect ratio of the ellipsoids in particular, but a larger error remains than in the previous cases with exact material parameters.

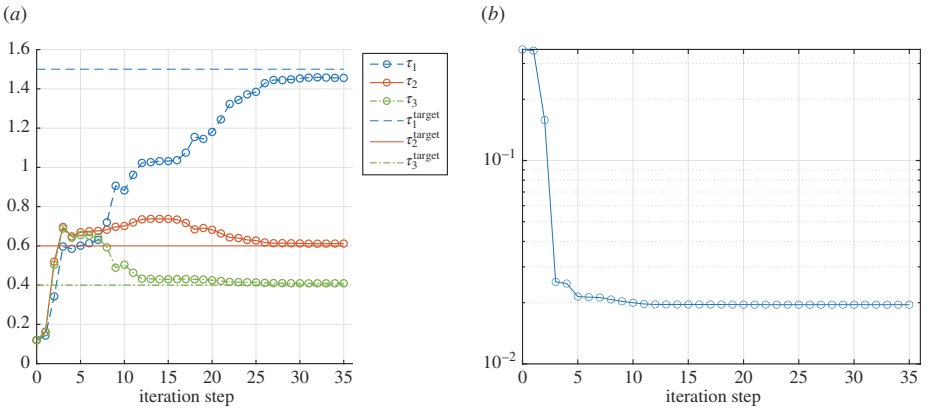

Figure 5. (*a*) Values of $\tau = (\tau_1, \tau_2, \tau_3)$ in each iteration step as well as target values (horizontal lines) in the third numerical experiment, which includes 3% noise added to the measured data. (*b*) Corresponding values of the target functional in each iteration step plotted on a semi-logarithmic scale.

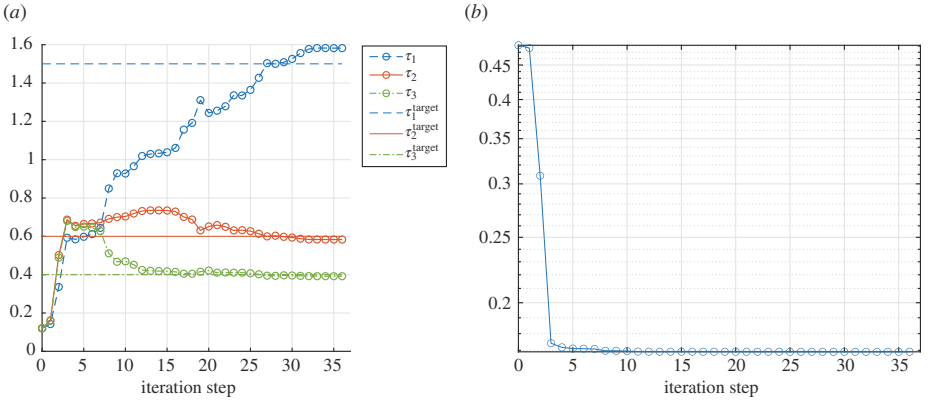

Figure 6. (*a*) Values of $\tau = (\tau_1, \tau_2, \tau_3)$ in each iteration step as well as target values (horizontal lines) in the fourth numerical experiment, which includes 9% noise added to the measured data. (*b*) Corresponding values of the target functional in each iteration step plotted on a semi-logarithmic scale.

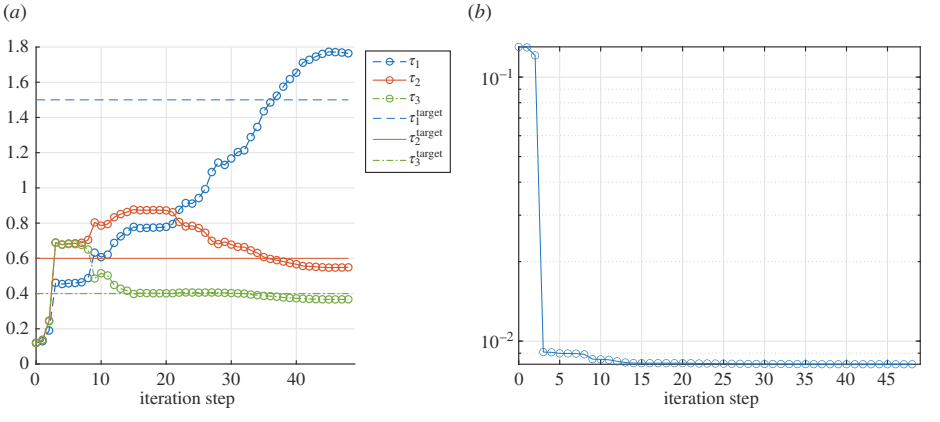

Figure 7. (*a*) Values of $\tau = (\tau_1, \tau_2, \tau_3)$ in each iteration step as well as target values (horizontal lines) in the fifth numerical experiment, which includes 3% noise added to the measured data as well as the material parameters. (*b*) Values of the target functional in each iteration step plotted on a semi-logarithmic scale.

Summing up, the results of the simulations show that we achieve a good approximation of the target value τ^{target} at the end of the iteration in the case of full information and exact measured data but also in the cases of only partial information or even noisy data. Reasonable results are still obtained if only noisy data based on noisy material parameters are available, all of which demonstrate the functioning of the method. As we considered only five test cases, a proper stability and sensitivity analysis, which is beyond the scope of this work, would be required to quantify this properly.

5. Conclusion

We considered the homogenized problem of the wave equation in a bounded domain in the context of linear elasticity in the long-wavelength regime, in which the microstructure is accounted for by the effective elasticity tensor, the elements of which are based on solutions of elliptic cell problems in the representative cell, as well as an effective mass obtained by direct averaging. We proved that there exists at least one solution of the corresponding inverse problem identifying geometrical information of the parametrized microstructure from macroscopic boundary measurements. With the formula (3.19) for the Gâteaux derivative of $\mathcal{J}$, wherefore we have to compute the shape derivative of the homogenized tensor and solve several weak wave problems, we were able to apply standard numerical gradient-based algorithms to obtain a solution to the minimization problem when measured data are given. Numerical experiments for an ellipsoidal microstructure illustrated that the length of the axes of the ellipsoids could be recovered from boundary measurements, even in the cases where measured data are only available on some faces of the sample and that the measured data are polluted by noise. The framework we developed appears to be generalizable to more advanced microscopic models, e.g. linear elasticity with slip-displacement conditions [25], and it would be of particular interest to extend it to microstructures dependent on the macroscopic variable, e.g. to be able to detect locally different production errors in quality inspection, i.e. to consider τ as a function of x, which makes the optimization problem infinite-dimensional.

Data accessibility. This article has no additional data.

Declaration of AI use. We have not used AI-assisted technologies in creating this article.

Authors' contributions. T.L.: conceptualization, formal analysis, methodology, software, writing—original draft; M.A.P.: conceptualization, formal analysis, methodology, supervision, writing—original draft, writing—review and editing.

Both authors gave final approval for publication and agreed to be held accountable for the work performed therein.

Conflict of interest declaration. We declare we have no competing interests.

Funding. This work was supported by EPSRC grant no EP/R014604/1. Furthermore, M.A.P. thanks Clare Hall, University of Cambridge, for a visiting fellowship during which part of this research was undertaken.

Acknowledgements. M.A.P. would like to thank the Isaac Newton Institute for Mathematical Sciences, Cambridge, for support and hospitality during the MWS programme where work on this paper was undertaken.

References

1. Lochner T, Peter MA. 2023 Identification of microstructural information from macroscopic boundary measurements in steady-state linear elasticity. *Math. Methods Appl. Sci.* **46**, 1295–1316. (doi:10.1002/mma.8581)
2. Orlik J, Panasenko G, Shiryaev V. 2016 Optimization of textile-like materials via homogenization and beam approximations. *Multiscale Model. Simul.* **14**, 637–667. (doi:10.1137/15M1017193)

3. Allaire G, Geoffroy-Donders P, Pantz O. 2019 Topology optimization of modulated and oriented periodic microstructures by the homogenization method. *Comput. Math. Appl.* **78**, 2197–2229. (doi:10.1016/j.camwa.2018.08.007)
4. Michailidis G. 2014 *Manufacturing constraints and multi-phase shape and topology optimization via a level-set method*. Doctoralthesis ecole polytechnique X. See https://pastel.archives-ouvertes.fr/pastel-00937306.
5. Allaire G, Jouve F, Van Goethem N. 2011 Damage and fracture evolution in brittle materials by shape optimization methods. *J. Comput. Phys.* **230**, 5010–5044. (doi:10.1016/j.jcp.2011.03.024)
6. Fallahpour M, Harbrecht H. 2023 Shape optimization for composite materials in linear elasticity. *Optim. Eng.* **24**, 2115–2143. (doi:10.1007/s11081-022-09768-7)
7. Herter C, Schöps S, Wollner W. 2023 Eigenvalue optimization with respect to shape-variations in electromagnetic cavities. *Proc. Appl. Math. Mech.* **22**, e202200122. (doi:10.1002/pamm.202200122)
8. Lochner T. 2022 *Homogenization and parameter identification of multiscale problems of linearized elasticity*. Germany: PhD dissertation Universität Augsburg.
9. Bonnet M, Cornaggia R, Guzina BB. 2018 Microstructural topological sensitivities of the second-order macroscopic model for waves in periodic media. *SIAM J. Appl. Math.* **78**, 2057–2082. (doi:10.1137/17M1149018)
10. Bonnet M, Guzina BB. 2009 Elastic-wave identification of penetrable obstacles using shape-material sensitivity framework. *J. Comput. Phys.* **228**, 294–311. (doi:10.1016/j.jcp.2008.09.009)
11. Cakoni F, Guzina BB, Moskow S. 2016 On the homogenization of a scalar scattering problem for highly oscillating anisotropic media. *SIAM J. Math. Anal.* **48**, 2532–2560. (doi:10.1137/15M1018009)
12. Cakoni F, Guzina BB, Moskow S, Pangburn T. 2019 Scattering by a bounded highly oscillating periodic medium and the effect of boundary correctors. *SIAM J. Appl. Math.* **79**, 1448–1474. (doi:10.1137/19M1237089)
13. Grosse C, Ochtsu M. 2008 *Acoustic emission testing: basic for research-applications in civil engineering*. Berlin, Germany: Springer.
14. Sause MGR. 2016 *In situ monitoring of fiber-reinforced composites: theory, basic concepts, methods, and applications. springer series in materials science*. Cham, Switzerland: Springer International Publishing. (doi:10.1007/978-3-319-30954-5)
15. Allaire G. 2002 *Shape optimization by the homogenization method*. New York: Springer. (doi:10.1007/978-1-4684-9286-6)
16. Delfour MC, Zolésio JP. 2011 Shapes and geometries. In *Metrics, analysis, differential calculus, and optimization*. (doi:10.1137/1.9780898719826). See http://epubs.siam.org/doi/book/10.1137/1.9780898719826.
17. Isakov V. 1998 *Inverse problems for partial differential equations*. New York: Springer. (doi:10.1007/978-1-4899-0030-2)
18. Kirsch A. 2011 *An introduction to the mathematical theory of inverse problems*. New York: Springer. (doi:10.1007/978-1-4419-8474-6)
19. Schweizer B. 2018 *Partielle Differentialgleichungen*. Berlin: Springer. (doi:10.1007/978-3-662-56668-8)
20. Cioranescu D, Damlamian A, Griso G. 2018 *The periodic unfolding method*. Singapore: Springer. (doi:10.1007/978-981-13-3032-2)
21. Bernard JME. 2011 Density results in sobolev spaces whose elements vanish on a part of the boundary. *Chin. Ann. Math. Ser. B* **32**, 823–846. (doi:10.1007/s11401-011-0682-z)
22. Henrot A, Pierre M. 2005 *Variation et optimisation de formes*. Berlin Heidelberg: Springer. (doi:10.1007/3-540-37689-5)
23. Gajewski H, Gröger K, Zacharias K. 1974 *Nichtlineare Operatorgleichungen und Operatordifferentialgleichungen*. Berlin. (doi:10.1515/9783112717899)
24. COMSOL. 2020 COMSOL multiphysics® version 5.6.COMSOL AB, Stockholm, Sweden. See https://www.comsol.com/release/5.6.
25. Lochner T, Peter MA. 2020 Homogenization of linearized elasticity in a two-component medium with slip displacement conditions. *J. Math. Anal. Appl.* **483**, 123648. (doi:10.1016/j.jmaa.2019.123648)